

Mottness in High-Temperature Copper-Oxide Superconductors

Philip Phillips^a, Ting-Pong Choy and Robert G. Leigh

Department of Physics, University of Illinois 1110 W. Green Street, Urbana, IL 61801, U.S.A

E-mail: ^adimer@uiuc.edu

Abstract. The standard theory of metals, Fermi liquid theory, hinges on the key assumption that although the electrons interact, the low-energy excitation spectrum stands in a one-to-one correspondence with that of a non-interacting system. In the normal state of the copper-oxide high-temperature superconductors, drastic deviations from the Fermi liquid picture obtain, highlighted by a pseudogap, broad spectral features and T -linear resistivity. A successful theory in this context must confront the highly constraining scaling argument which establishes that all 4-Fermi interactions are irrelevant (except for pairing) at a Fermi surface. This argument lays plain that new low-energy degrees of freedom are necessary. This article focuses on the series of experiments on the copper-oxide superconductors which reveal that the number of low-energy addition states per electron per spin exceeds unity, in direct violation of the key Fermi liquid tenet. These experiments point to new degrees of freedom, not made out of the elemental excitations, as the key mechanism by which Fermi liquid theory breaks down in the cuprates. A recent theoretical advance which permits an explicit integration of the high energy scale in the standard model for the cuprates reveals the source of the new dynamical degrees of freedom at low energies, a charge $2e$ bosonic field which has nothing to do with pairing but rather represents the mixing with the high energy scales. We demonstrate explicitly that at half-filling, this new degree of freedom provides a dynamical mechanism for the generation of the charge gap and antiferromagnetism in the insulating phase. At finite doping, many of the anomalies of the normal state of the cuprates including the pseudogap, T -linear resistivity, and the mid-infrared band are reproduced. A possible route to superconductivity is explored.

1. Introduction

Superconductivity in the copper-oxide ceramics stands as a grand challenge problem as its solution is fundamentally rooted in the physics of strong coupling. In such problems, traditional calculational schemes based on the properties of single free particles fail. Rather the physics of strong coupling resides in collective behaviour, signified typically by the emergence of new degrees of freedom at low energy. For example, in quantum-chromodynamics (QCD) the propagating degrees of freedom in the infrared (IR) are bound states not related straightforwardly to the ultra-violet (UV) scale physics. The key perspective presented here is that similar physics stems from the strong electron interactions in the copper-oxide superconductors. We will delineate precisely how the emergence of collective behaviour at low energy accounts for many of the anomalous properties of the normal state of the cuprates.

That the cuprates embody strong coupling physics stems from the Mott insulating[1] nature of the parent state. Such materials possess a half-filled band but insulate, nonetheless. Their insulating behaviour derives from the large on-site interaction two opposite-spin electrons encounter whenever they doubly occupy the same lattice site. For the cuprates[2], the on-site electron repulsion is typically $U \simeq 4eV$ whereas the nearest-neighbour hopping matrix element is only $t \simeq 0.4eV$. Although double occupancy is costly, there is no symmetry principle that forbids it even at half-filling. In the original proposal by Mott[1] to explain why NiO insulated, he assumed, as illustrated in Fig. (1), that each Ni atom remained neutral because

$$U = E^{N+1} + E^{N-1} - 2E^N \quad (1)$$

dominates all other energy scales. Here E^N is the ground state energy of an atom with N valence electrons. For each Ni atom, $N = 2$. Hence, the zero-temperature state envisioned by Mott is one in which no atom is excited with an occupation of $N \pm 1$ electrons. For NiO, this translates to no Ni^{+++} or Ni^+ ions exist as explicitly stated by Mott[1]. However, it is well-known[3, 4, 5] that the ground state of a Mott insulator possesses doubly occupied sites at half-filling. As a result, the simple cartoon[1] that the Mott gap originates because double occupancy is forbidden is incomplete. Some have advocated[6] that in the Mott insulator, doubly occupied sites are immobile whereas in the metal they form a fluid. This account requires an explicit dynamical mechanism for the generation of the Mott gap. However, the dynamical degrees of freedom leading to the localization of double occupancy have not been unearthed. We offer here an explicit resolution of this problem.

A few of the properties of doped Mott insulators are sketched in the phase diagram in Fig. (2). Aside from $d_{x^2-y^2}$ superconductivity, the pseudogap, in which the single-particle density of states is suppressed[7, 8, 13], and the strange metal, characterised by the ubiquitous T -linear resistivity[14, 15], stand out. As the phase diagram suggests, the pseudogap and strange metal phases are intimately related. That is, a correct theory of the pseudogap state of matter should at higher temperatures yield a metallic phase in which the resistivity scales as a linear function of temperature.

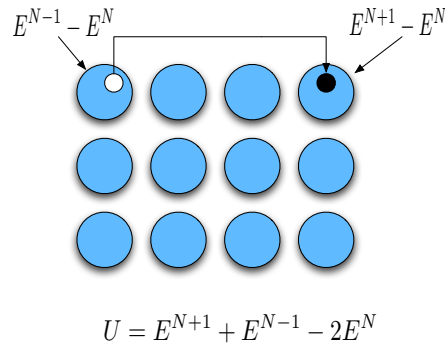


Figure 1. A half-filled band as envisioned by Mott. Each blue circle represents a neutral atom with N electrons and ground-state energy E^N . The energy differences for electron removal and addition are explicitly shown. Mott reasoned that no doubly occupied sites exist because at zero temperature, $U = E^{N+1} + E^{N-1} - 2E^N \gg 0$. This is, of course, not true. As a consequence the Mott gap must be thought of dynamically rather than statically.

Nonetheless, numerous proposals[16, 17, 18, 19, 20, 21, 22] for the pseudogap abound that offer no resolution of T -linear resistivity. Part of the problem is that a series of associated phenomena, for example, incipient diamagnetism[23] indicative of incoherent pairing[20, 21, 22, 24], electronic inhomogeneity[25, 26, 27, 28, 29, 16], time-reversal symmetry breaking[30, 31, 32, 33], and quantum oscillations[34] in the Hall conductivity, possibly associated with the emergence of closed electron (not hole) pockets in the first Brillouin zone (FBZ), obscure the efficient cause of the pseudogap and its continuity with the strange metal. Despite this range of phenomena, a key experimental measure[15, 35] of the pseudogap onset is the temperature, T^* , at which the first deviation from T -linear resistivity obtains. As a consequence, the physics underlying the strange metal must also yield a pseudogap at lower temperatures. Further, it must do so in a natural way. In our work, we take the relationship between the strange metal and pseudogap seriously and develop a theory[9, 10, 11] that explains both simultaneously. In addition, we show that the same theory is capable of explaining other anomalies of the normal state such as 1) absence of quasiparticles[12] in the normal state, 2) the mid-infrared band in the optical conductivity[36, 37, 38, 39, 40, 41], 3) spectral weight transfer across the Mott gap, and 4) the high and low-energy kinks in the electron removal spectrum.

While it has been acknowledged for some time[42] that the normal state of the cuprates is incompatible with Fermi liquid theory, precisely what replaces it has not been settled. In a Fermi liquid, the low-energy excitation spectrum stands in a one-to-one correspondence with that of a non-interacting system. This correspondence must clearly break down in the normal state of the cuprates. The arguments of Polchinski[42] and others[43, 44, 45] make it clear that breaking Fermi liquid theory in $d = 2$ requires new degrees of freedom at low energy, not simply 4-fermion interactions as they are all (except for pairing) irrelevant at the Fermi liquid fixed point. One possible origin of the new degrees of freedom[46] is if spectral weight transfer between high and low energies

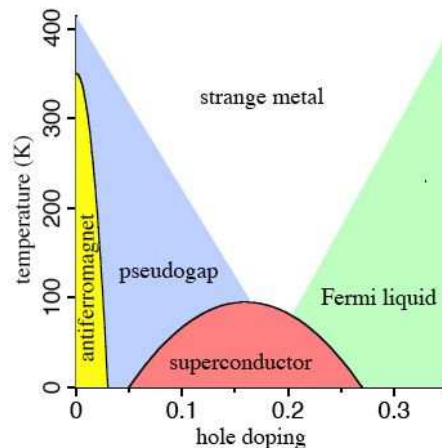


Figure 2. Heuristic phase diagram of the copper-oxide superconductors. In the strange metal, the resistivity is a linear function of temperature. In the pseudogap the single-particle density of states is suppressed without the onset of global phase coherence indicative of superconductivity. As discussed in Section 3.6, the dome-shape of the superconducting region with an optimal doping level of $x_{\text{opt}} \approx 0.17$ is not quantitatively accurate. See Fig. 19 for a more accurate determination of x_{opt} .

mediates new electronic states at low energy. As a result, new states will emerge at low energy that have no counterpart in the non-interacting system. We show quite generally that this state of affairs obtains in the minimal model for a doped Mott insulator, namely the Hubbard model. Refinements of this model to include more details of the copper-oxide plane also retain this feature. We establish this result first through a simple physical argument which lays plain that in a doped Mott insulator, the phase space available for adding a particle exceeds the number of ways electrons can be added at low energy. Consequently, some new degrees of freedom not made out of the elemental excitations must reside in the low-energy spectrum. By explicitly integrating out the degrees of freedom far away from the chemical potential, the Wilsonian program for constructing a proper low-energy theory, we show that this new excitation is a charge $2e$ bosonic field that in no way has anything to do with pairing. It is from this new degree of freedom that the pseudogap and T-linear resistivity follow immediately. Since this physics arises without any appeal to some further fact but relies only on the strong correlations of the doped Mott state, we have successfully isolated the efficient cause of the pseudogap. The associated phenomena mentioned above are supervenient on rather than central to the physics of the normal state. This review is organised as follows. In the next section, we discuss the experimental evidence for spectral weight transfer and show that it requires new degrees of freedom at low energy not made out of the elemental excitations. In section II, we derive the exact low-energy theory by formally integrating out the degrees of freedom far away from the chemical potential. In Section III, we compare the predictions of the theory with experiment. We close with a perspective on the remaining problem of superconductivity.

2. Mottness

The origin of the Mott insulating state is subtle for two related reasons. First, the Mott gap cannot be easily deduced from the bare degrees of freedom in a model Hamiltonian. As remarked in the introduction, even in the Hubbard model, the ground state contains admixtures with the degrees of freedom, namely double occupancy, that lie above the gap. That is, if one were to write the bare electron operator[3]

$$c_{i\sigma} = (1 - n_{i-\sigma})c_{i\sigma} + n_{i-\sigma}c_{i\sigma} \quad (2)$$

as a sum of two operators, one of which vanishes on doubly occupied sites, $\xi_{i\sigma} = (1 - n_{i-\sigma})c_{i\sigma}$ and its complement which is only non-zero when a site is doubly occupied, $\eta_{i\sigma} = n_{i-\sigma}c_{i\sigma}$, one would see immediately that such a separation is not canonical. As a result, $\eta_{i\sigma}$ and $\xi_{i\sigma}$ have a non-zero overlap and hence they do **not** propagate independently as would be required for them to be gapped. In fact, it is unclear precisely how to write down a set of canonically defined fermionic operators that do become gapped as a result of the energy cost for double occupancy. This is the Mott problem. Its persistence has led Laughlin[47] to assert that the Mott problem is fictitious and, in reality, does not exist. As mentioned in the preceding section, the real problem is that the Mott gap is fundamentally dynamical in nature. That it is difficult to write down the precise degrees of freedom that are becoming gapped is just a symptom of this fact. As will become clear from this review, the dynamical degrees of freedom that ultimately produce the Mott gap only appear when the high-energy scale is integrated out exactly.

Second, all known Mott insulators order antiferromagnetically at sufficiently low temperature. To illustrate, two electrons on neighbouring sites with opposite spins can exchange their spins. This process proceeds through an intermediate state in which one of the sites is doubly occupied and hence the corresponding matrix element scales as t^2/U . Antiferromagnetism in the cuprates arises from this mechanism. This mechanism is distinct from the weak-coupling Slater[48] process in which a half-filled band orders as a result of nesting at $Q = (\pi, \pi)$. While antiferromagnetism is certainly part of the Mott insulating story, it leaves much unexplained. It is that explanatory residue, namely the properties of Mott insulators which do not necessitate ordering, we refer to as *Mottness*. A simple property unexplained by ordering is the Mott gap itself. Above any temperature associated with ordering, an optical gap obtains[36, 37, 49]. Another such property is spectral weight transfer.

2.1. Spectral Weight Transfer

While what constitutes the minimal model for the cuprates can certainly be debated, it is clear[50, 51, 52] that regardless of the model, the largest energy scale arises from doubly occupying the copper $d_{x^2-y^2}$ orbital. This orbital can hybridise with the in-plane p_x and p_y orbitals and hence a two-band model is natural. Since our emphasis is on the interplay between the high and low-energy scales, we simplify to a one-band Hubbard[3]

model

$$H_{\text{Hubb}} = -t \sum_{i,j,\sigma} g_{ij} c_{i,\sigma}^\dagger c_{j,\sigma} + U \sum_{i,\sigma} c_{i,\uparrow}^\dagger c_{i,\downarrow}^\dagger c_{i,\downarrow} c_{i,\uparrow}, \quad (3)$$

where i, j label lattice sites, g_{ij} is equal to one iff i, j are nearest neighbours, $c_{i\sigma}$ annihilates an electron with spin σ on lattice site i , t is the nearest-neighbour hopping matrix element and U the energy cost when two electrons doubly occupy the same site. Our conclusions carry over naturally to any n-band model of the cuprates as long as the largest energy scale is the on-site energy, U in Eq. (3). That the dynamics of the charge carriers in the cuprates are captured by this model was confirmed by Oxygen 1s x-ray absorption[53] on $\text{La}_{2-x}\text{Sr}_x\text{CuO}_4$. In such experiments, an electron is promoted from the core 1s to an unoccupied level. The experimental observable is the fluorescence yield as a function of energy as electrons relax back to the valence states. The experiments, Fig. (3), show that at $x = 0$, all the available states lie at 530eV. As a function of doping, the intensity in the high-energy peak decreases and is transferred to states at 528eV. In fact, the lower peak grows faster than $2x$ while the upper peak decreases faster than $1 - x$. The separation between these two peaks is the optical gap in the parent insulating material. Though this observation of transfer of spectral weight from high to low energy is not expected in a semiconductor or a band insulator, it is certainly not an anomaly in strongly correlated systems. In fact, it is the fingerprint of Mottness as it has been observed in the classic Mott system NiO upon Li doping[49] and in all optical conductivity measurements on the cuprates[36, 37, 39, 40, 41] above any temperature having to do with ordering.

This generic behaviour of spectral weight transfer is captured by the Hubbard model. To illustrate, consider the half-filled Hubbard model. A charge gap splits the spectrum into two parts, lower and upper Hubbard bands. Roughly, the lower Hubbard band (LHB) describes particle motion on empty sites while particle motion on already singly occupied sites is captured by the upper Hubbard band (UHB). This relationship is only approximate because the UHB and LHB are mixed so that there are states in the LHB that have some doubly occupied character. To understand spectral weight transfer, we start in the atomic limit in which there is a clean gap of order U between the UHB and LHB. For a system containing N electrons on N sites, the weight of the LHB is N corresponding to N ways to remove an electron. The corresponding weight in the UHB is N as well as there are N ways to add an electron to the system. These bands are shown in Fig. (4). Consequently, adding a hole in the atomic limit decreases the electron removal spectrum in the LHB by one state. The weight in the UHB is also affected as there are now $N-1$ ways to create a doubly occupied site. This leaves two states unaccounted for. The two extra states are part of the addition spectrum at low energies and correspond to the two ways of occupying the empty site by either a spin up or a spin down electron. In the atomic limit, the number of addition states scales as $2x$ [54, 55] when x holes are created. In a semiconductor or a Fermi liquid, the number of addition states would be strictly x . Experimentally[53, 49, 36, 37, 39, 40, 41], however, the low-energy spectral weight (LESW) grows faster than $2x$. The excess of $2x$

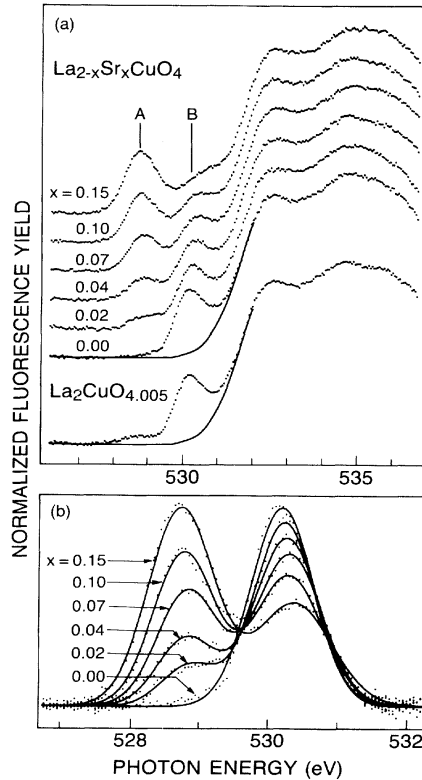


Figure 3. a) Normalized fluorescence[53] yield at the O K edge of $\text{La}_{2-x}\text{Sr}_x\text{CuO}_{4+\delta}$. In the undoped sample, the only absorption occurs at 530eV, indicated by B. Upon doping the intensity at B is transferred to the feature at A, located at 528eV. b) Gaussian fits to the absorption features at A and B with the background subtracted. Reprinted from Chen, et al. Phys. Rev. Lett. **66**, 104 (1991).

can be understood simply by turning on the hopping[4]. When the hopping is non-zero, empty sites are created as a result of the creation of double occupancy. Such events increase the number of available states for particle addition and as a consequence the LESW increases faster than $2x$. It is important to recall that the argument leading to the LESW exceeding $2x$ relies on the strong coupling limit. If this limit is not relevant to the ground state at a particular filling, the previous argument fails.

2.2. Breakdown of Fermi Liquid Theory: More than just Electrons

A natural question arises. Is spectral weight transfer important? A way of gauging importance is to determine if spectral weight transfer plays any role in a low-energy theory. A low-energy theory is properly considered to be natural if there are no relevant perturbations. Several years ago, Polchinski[42] and others[43, 44, 45] considered Fermi liquid theory from the standpoint of renormalisation. They found[42, 43, 44, 45] that as long as one posits that the charge carriers are electrons, there are no relevant interactions (except for pairing) that destroy the Fermi liquid state. The setup[42] is as follows. Decompose the momenta into the Fermi momentum and a component orthogonal to

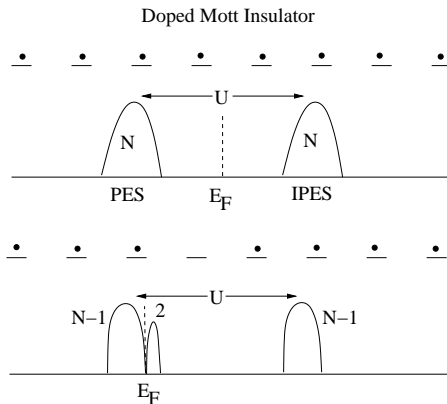


Figure 4. Evolution of the single-particle density of states from half-filling to the one-hole limit in a doped Mott insulator described by the Hubbard model. Removal of an electron results in two empty states at low energy as opposed to one in the band-insulator limit. The key difference with the Fermi liquid is that the total weight spectral weight carried by the lower Hubbard band (analogue of the valence band in a Fermi liquid) is not a constant but a function of the filling.

the Fermi surface

$$\mathbf{p} = \mathbf{k} + \ell. \quad (4)$$

Here \mathbf{l} is the component orthogonal to the Fermi surface. Then consider scaling of energy and momentum towards the Fermi surface, in other words

$$E \rightarrow uE, \quad \mathbf{k} \rightarrow \mathbf{k}, \quad \ell \rightarrow u\ell, \quad (5)$$

where u is the scaling parameter. To quadratic order, the action is

$$S = \int dt d^3\mathbf{p} [i\psi^*(\mathbf{p})\partial_t\psi(\mathbf{p}) - (E(\mathbf{p}) - E_F(\mathbf{p}))\psi^*(\mathbf{p})\psi(\mathbf{p})].$$

Hence, close to the Fermi surface

$$E(\mathbf{p}) - E_F(\mathbf{p}) \sim \ell v_f, \quad v_F = \partial_{\mathbf{p}}E \quad (6)$$

so that after scaling towards the Fermi surface (note that also $t \rightarrow u^{-1}t$) one finds that

$$\psi \rightarrow u^{-1/2}\psi. \quad (7)$$

Consider now the four-fermion interaction. The argument to show that such interactions are irrelevant is particularly simple. In terms of powers of the scaling parameter, u , the measure over time contributes one negative power, the measure over the momenta orthogonal to the Fermi surface 4 powers and the 4-fermi interaction $4/2$ negative powers. The delta function over the 4-momenta generically does not scale. Hence, the overall scaling of the four-Fermi interaction is governed by $u^{-1+4-4/2} = u^1$ and hence is irrelevant as the power of u is positive. The only exception to this argument if inversion symmetry is present is the Cooper pairing interaction. Consequently, as long as the charge carriers carry unit charge, there are no relevant interactions that destroy Fermi liquid theory. In the context of the cuprates, this argument is particularly powerful as it implies that in order to explain T -linear resistivity, some new emergent degrees of

freedom that have nothing to do with the electrons must be present. There have been attempts to circumvent this argument in the literature that amount to essentially free field theory. In light of the above argument, such attempts must reduce to Fermi liquid theory and hence must yield T^2 resistivity. Others[56, 57] have directly confronted the Polchinski[42] argument and added extra derivative couplings to the Fermi liquid action. However, the relationship of such continuum models[56, 57] to any concrete realisation of Mott physics is not clear.

It is straightforward to show that dynamical spectral weight transfer in a doped Mott insulator leads to a breakdown of the Fermi liquid picture and the emergence of new low-energy degrees of freedom. The interactions of the electrons with the new degrees of freedom can be formulated as a natural theory in which the electron spin-spin interaction is sub-dominant. As will be seen, the interactions with the new degrees of freedom govern all the physics that is independent of ordering. In this sense, we arrive at a natural separation between spin-ordering and Mott physics. To proceed, we define the number of single-particle addition states per site at low energy,

$$L = \int_{\mu}^{\Lambda} N(\omega) d\omega, \quad (8)$$

as the integral of the single-particle density of states ($N(\omega)$) from the chemical potential, μ , to a cutoff energy scale, Λ , demarcating the IR and UV scales. As long as Λ is chosen to exclude the high-energy scale, L is a well-defined quantity which simply counts the number of states in the unoccupied part of the spectrum at low energy. We compare this quantity to the number of ways an electron can be added to the holes created by the dopants. We call this quantity n_h . Our usage of ‘ways’ here refers to the spin degree of freedom of the electron only and not to combinatorics. From the perspective of single-particle physics, the intensity of a band is always equal to the number of electrons the band can hold. Hence, strict adherence to the single-particle picture requires that $L = n_h$, implying that the number of low-energy addition states per electron per spin is identically unity. For example, as shown in Fig. (5), in a non-interacting system, $L = 2 - n = n_h$. The same is true for a Fermi liquid as can be seen from the fact that

$$\int_{-\infty}^{\epsilon_F} N(\omega) d\omega = n. \quad (9)$$

Since the integral over all energies must yield 2, it follows that $L = 2 - n$. Hence, strictly for a Fermi liquid, $L/n_h = 1$ as is dictated by the basic Landau tenet that the number of bare electrons at a given chemical potential equals the number of Fermi excitations (quasiparticles) in the interacting system.

A doped Mott system is quite different because the total spectral weight in the lower-Hubbard band is not simply 2 but rather determined by the electron filling. Consider a Mott system in the atomic limit. As shown in the previous section, $L = 2x$ is the exact result in the atomic limit because creating a hole leaves behind an empty site which can be occupied by either a spin-up or a spin-down electron. Likewise, the number of ways electrons can occupy the empty sites is $n_h = 2x$. Hence, even in the atomic limit of a doped Mott insulator, $L/n_h = 1$. However, real Mott systems are not

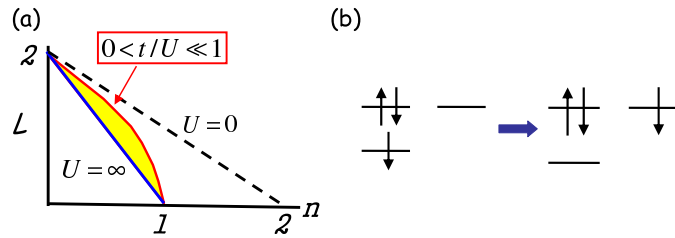


Figure 5. a) Integrated low-energy spectral weight, L , defined in Eq. (5), as a function of the electron filling, n : 1) the dashed line is the non-interacting limit, vanishing on-site interaction ($U = 0$), in which $L = 2 - n$, 2) atomic limit (blue line) of a doped Mott insulator, $U = \infty$, in which $L = 2(1 - n) = 2x$, x the doping level and 3) a real Mott insulator in which $0 < t/U \ll 1$, red curve. For $0 < t/U \ll 1$, L must lie strictly above the $U = \infty$ limit and hence $L > 2x$ away from the atomic limit. (b) Hopping processes mediated by the t/U terms in the expansion of the projected transformed operators in terms of the bare electron operators (see Eq. (16)). As a result of the t/U terms in Eq. (16), the low-energy theory in terms of the bare fermions does not preserve double occupancy. The process shown here illustrates that mixing between the high and low-energy scales obtains only if double occupancy neighbours a hole. In the exact low-energy theory, such processes are mediated by the new degree of freedom, φ_i , the charge $2e$ bosonic field which binds a hole and produces a new charge e excitation, the collective excitation in a doped Mott insulator.

in the atomic limit. In strong coupling, finite hopping with matrix element t creates double occupancy, and as a result empty sites with weight t/U . Such empty sites with fractional weight contribute to L as shown first by Harris and Lange[4]. In fact, every order in perturbation theory contributes to L . Consequently, when $0 < t/U \ll 1$, L is strictly larger than $2x$. Such hopping processes or quantum fluctuations do not affect the number of electrons that can be added to the system, however. Since n_h remains fixed at $2x$, in a real doped Mott system, $L/n_h > 1$. Consequently, in contrast to a Fermi liquid, simply counting the number of electrons that can be added does *not* exhaust the available phase space to add a particle at low energy. That is, addition states that do not have the quantum numbers of an electron must exist as illustrated in Fig. (6). Since the number of ways of adding a particle exceeds the number of electrons that can be added, the additional states must be gapped to the addition of an electron. This gap can manifest itself straightforwardly as a depression in the density of states at the chemical potential or more subtly as a reconstruction[58] of the non-interacting Fermi surface, for example, one that has electron (or hole) pockets that shrink in size as the doping decreases. Numerical simulations show[59] that such reconstructions do not necessitate broken symmetry but obtain entirely from the strong correlations in a doped Mott insulator. In either case, the one-to-one correspondence between the excitation spectrum in the free and interacting systems breaks down. In doped Mott systems, this breakdown arises entirely from spectral weight transfer. While it has been known for some time[4] that $L > 2x$ at strong coupling in a doped Mott insulator based on the Hubbard model, that this simple fact implies a pseudogap (whose dimensional dependence is discussed in Section 3.2) has not been deduced previously. Thus, additional degrees of freedom at

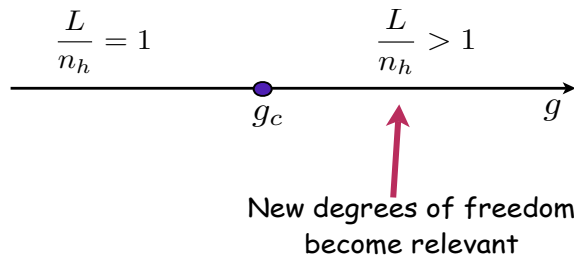


Figure 6. Schematic depiction of electronic models based on the magnitude of L/n_h . In a Fermi liquid, $L/n_h = 1$. $L/n_h > 1$ necessarily leads to a break down of the Fermi liquid picture as new degrees of freedom not made out of the electrons are needed. $L/n_h > 1$ appears to be the generic way in which Fermi liquid theory breaks down in a doped Mott insulator.

low-energy, not made out of the elemental excitations, emerge in a low-energy reduction of a doped Mott insulator at strong coupling. Note, it is only the spectral weight in excess of $2x$ that creates the new physics. Hence, the physics governed by the new degrees of freedom has nothing to do with gauge[60, 61, 62] fields that engineer the no double occupancy constraint in standard treatments of doped Mott insulators. The physics referred to here is precisely the part thrown away in such treatments. We refer to this contribution as the dynamical part of the spectral weight. This dynamical part of L arises through exchanges with doubly occupied sites. Hence, although t/U is approximately $1/10$ in the cuprates, the t/U corrections to L must be retained as they mediate fundamentally new physics that is quantifiable. Namely, it is through these corrections that a Fermi liquid description breaks down as depicted in Fig. (6). As a result, one might imagine that the new physics is associated with some new collective excitation with charge $2e$. The new theory we construct, in which we integrate out exactly the high energy scale, has such a degree of freedom which does in fact mediate the dynamical part of L . In light of Polchinski's argument[42], any non-Fermi liquid behaviour must emerge from the new collective charge $2e$ excitation. We show that this is in fact the case.

2.3. Perturbative Approaches

It is possible to account for the dynamical contribution to the low-energy spectral weight using degenerate perturbation theory. While this method does not shed any light on the missing degree of freedom at low energy, it does serve to illustrate that the limits of $U \rightarrow \infty$ and the thermodynamic limit, $N \rightarrow \infty$, do not commute. In fact, it is this lack of commutativity that gives rise to $L > 2x$. We review this method here as it does serve to motivate our eventual analysis.

The goal of perturbative approaches[63, 64, 65, 66, 67, 68] in this context is to bring the Hubbard model into diagonal form with respect to double occupancy. As with any matrix diagonalization problem, the new basis which makes double occupancy a good

quantum number involves some linear combination of the old states. The subtlety that this introduces is that the no double-occupancy condition applies only to the transformed fermions **not** to the original bare electrons. This is an oft-overlooked fact that has led to much confusion over what precisely the accepted low-energy reduction of the Hubbard model, namely the t-J model[69], entails. We review the derivation with an eye on isolating the processes which lead to dynamical spectral weight transfer. Let $f_{i\sigma}$ be the dressed operators which make the Hubbard model block diagonal with respect to ‘‘double occupancy.’’ Following Eskes et al.[63], for any operator O , we define \tilde{O} such that $O \equiv \mathbf{O}(c)$ and $\tilde{O} \equiv \mathbf{O}(f)$, simply by replacing the Fermi operators $c_{i\sigma}$ with the transformed fermions $f_{i\sigma}$. To block diagonalise the Hubbard model,

$$H[f] \equiv e^{S[f]} \tilde{H}[f] e^{-S[f]}, \quad (10)$$

one constructs a similarity transformation $S[f]$ which connects sectors that differ by at most one ‘fictive’ doubly occupied site, that is, a doubly occupied site in the transformed basis. To lowest order,

$$S^{(1)} = \frac{1}{U} (\tilde{T}_{+1} - \tilde{T}_{-1}). \quad (11)$$

where

$$\tilde{T}_{+1} = -t \sum_{i,j,\sigma} g_{ij} \tilde{n}_{i\bar{\sigma}} f_{i\sigma}^\dagger f_{j\sigma} (1 - \tilde{n}_{j\bar{\sigma}}), \quad (12)$$

which increases the quantum number $\tilde{V} = \sum_i \tilde{n}_{i\uparrow} \tilde{n}_{i\downarrow}$ by one. Likewise, $\tilde{T}_{-1} = (T_{+1})^\dagger$ decreases \tilde{V} by one. In the new basis, $[H, \tilde{V}] = 0$, implying that double occupation of the transformed fermions is a good quantum number, and all of the eigenstates can be indexed as such. This does not mean that $[H, V] = 0$. If it were, there would have been no reason to do the similarity transformation in the first place. \tilde{V} , and not V , is conserved. Assuming that V is the conserved quantity results in a spurious local SU(2)[70, 71] symmetry in the strong-coupling limit at half-filling.

To expose the dynamical contribution to spectral weight transfer, we focus on the relationship between the physical and transformed fermions. As expected in any degenerate perturbation scheme, the bare fermions,

$$c_{i\sigma} = e^S f_{i\sigma} e^{-S} \simeq f_{i\sigma} - \frac{t}{U} \sum_{\langle j,i \rangle} [(\tilde{n}_{j\bar{\sigma}} - \tilde{n}_{i\bar{\sigma}}) f_{j\sigma} - f_{j\bar{\sigma}}^\dagger f_{i\sigma} f_{i\bar{\sigma}} + f_{i\bar{\sigma}}^\dagger f_{i\sigma} f_{j\bar{\sigma}}], \quad (13)$$

are linear combinations of the multiparticle states in the transformed basis. We invert this relationship to find that

$$f_{i\sigma} \simeq c_{i\sigma} + \frac{t}{U} \sum_j g_{ij} X_{ij\sigma} \quad (14)$$

where

$$X_{ij\sigma} = [(n_{j\bar{\sigma}} - n_{i\bar{\sigma}}) c_{j\sigma} - c_{j\bar{\sigma}}^\dagger c_{i\sigma} c_{i\bar{\sigma}} + c_{i\bar{\sigma}}^\dagger c_{i\sigma} c_{j\bar{\sigma}}]. \quad (15)$$

Since the low energy theory is captured by the sector in the transformed basis which has no double occupancy, it is most relevant to focus on the form of the projected

transformed fermions. Using the relations above, we find that as expected, the projected transformed fermions

$$(1 - \tilde{n}_{i\bar{\sigma}})f_{i\sigma} \simeq (1 - n_{i\bar{\sigma}})c_{i\sigma} + \frac{t}{U}V_{\sigma}c_{i\bar{\sigma}}^{\dagger}b_i + \frac{t}{U}\sum_j g_{ij}[n_{j\bar{\sigma}}c_{j\sigma} + n_{i\bar{\sigma}}(1 - n_{j\bar{\sigma}})c_{j\sigma} + (1 - n_{j\bar{\sigma}})(c_{j\sigma}^{\dagger}c_{i\sigma} - c_{j\sigma}c_{i\sigma}^{\dagger})c_{i\bar{\sigma}}] \quad (16)$$

involve double occupancy in the bare fermion basis. Here $V_{\sigma} = -V_{\bar{\sigma}} = 1$ and $b_i = \sum_{j\sigma} V_{\sigma}c_{i\sigma}c_{j\bar{\sigma}}$ where j is summed over the nearest neighbors of i . The projected bare fermion, $(1 - n_{i\bar{\sigma}})c_{i\sigma}$, yields the $2x$ sum rule, whereas it is the admixture with the doubly occupied sector that mediates the t/U corrections. A process mediated by these terms is shown in Fig. (5). This can be seen more clearly by computing L directly using Eq. (13). The standard treatment[60, 61, 62, 69] of the t - J model ignores the dynamical corrections as a hard projection scheme is implemented in which the no double occupancy condition applies not only to the transformed but also to the bare fermions. As we have pointed out in the introduction, the physics left out by projecting out double occupancy is important because it tells us immediately that $L/n_h > 1$ as can be seen from the expression for L :

$$L \equiv 2\langle(1 - n_{i\uparrow})(1 - n_{i\downarrow})\rangle \quad (17)$$

$$= 2\langle(1 - \tilde{n}_{i\uparrow})(1 - \tilde{n}_{i\downarrow})\rangle + \frac{2t}{U}\sum_{i,j,\sigma} g_{ij}\langle f_{i\sigma}^{\dagger} [(\tilde{n}_{j\bar{\sigma}} - \tilde{n}_{i\bar{\sigma}})f_{j\sigma}f_{j\bar{\sigma}}^{\dagger}f_{i\sigma}f_{i\bar{\sigma}} + f_{i\bar{\sigma}}^{\dagger}f_{i\sigma}f_{j\bar{\sigma}}] (1 - \tilde{n}_{i\bar{\sigma}}) + h.c. \rangle \quad (18)$$

As is evident, $2\langle(1 - \tilde{n}_{i\uparrow})(1 - \tilde{n}_{i\downarrow})\rangle = 2x$ in the projected Hilbert space of the dressed fermions which corresponds to the $2x$ sum rule of the static part in the low energy spectral weight. The dynamical part of L arises from the t/U corrections. It is these corrections that prevent the operator in Eq. (16) from being regarded as a free excitation. Rather it describes a non-Fermi liquid ($L/n_h > 1$).

However, it is particularly cumbersome to extract physical insight from the canonical transformation method. The primary reason is that any information regarding the bare fermions requires that the similarity transformation be undone when any experimentally relevant quantity is calculated. Consider for example the electron spectral function. In the hard projected version of the $t - J$ model[60, 61, 62, 69], the electron spectral function is assumed to be given by simply the time-ordered anticommutator of the transformed fermions. However, Eq. (13) illustrates that this is not so. In actuality, the single-particle Green function,

$$G(\mathbf{k}, \omega) = -iFT\langle T c_{i\sigma} c_{j\sigma}^{\dagger} \rangle = -iFT\langle T f_{i\sigma} f_{j\sigma}^{\dagger} \rangle + iFT\frac{t}{U}\sum_k g_{ik}\langle T [(\tilde{n}_{k\bar{\sigma}} - \tilde{n}_{i\bar{\sigma}})f_{k\sigma}f_{k\bar{\sigma}}^{\dagger}f_{i\sigma}f_{i\bar{\sigma}} + f_{i\bar{\sigma}}^{\dagger}f_{i\sigma}f_{k\bar{\sigma}}] f_{j\sigma}^{\dagger} \rangle + iFT\frac{t}{U}\sum_k g_{jk}\langle T f_{i\sigma} [(\tilde{n}_{k\bar{\sigma}} - \tilde{n}_{j\bar{\sigma}})f_{k\sigma}f_{k\bar{\sigma}}^{\dagger}f_{j\sigma}f_{j\bar{\sigma}} + f_{j\bar{\sigma}}^{\dagger}f_{j\sigma}f_{k\bar{\sigma}}]^{\dagger} \rangle, \quad (19)$$

has t/U corrections in the transformed basis. Although these corrections are naively down by a factor of t/U relative to the projected part, their contribution cannot be ignored because it is in these corrections that the explicit non-Fermi liquid behaviour is hidden. To illustrate, all calculations on the $t - J$ model of the single hole problem[72, 73, 74, 75] in a quantum antiferromagnet yield a finite value of Z proportional to J/t . However, in the Hubbard model, the situation is not as clear. Simulations on finite-size systems reveal that $Z \propto L^{-\alpha}$ where $\alpha > 0$ and hence tends to zero as the system size increases. While this calculation is not conclusive, it is consistent with the fact that similar dynamical mean-field treatments of the t-J and Hubbard models at finite doping yield a finite conductivity as $T \rightarrow 0$ in the $t - J$ model[76, 77] but a vanishing value in the Hubbard model as $T \rightarrow 0$ [78]. These differences are summarized in Table (1). The most striking results in Table (1) are those for the exponents governing the asymptotic fall-off of the density correlations, α_c , and momentum distribution functions (θ) in the $t - J$ (with $t = J$, the supersymmetric point) and Hubbard models in $d = 1$. Here these quantities can be obtained exactly[79, 80, 81] for both models using Bethe ansatz. In the $d=1$ Hubbard model, the exponent θ approaches[80, 81] $1/8$ asymptotically as $U \rightarrow \infty$ for any filling. By contrast in the $t - J$ model[79], θ is strongly dependent on doping with a value of $1/8$ at half-filling and vanishing to zero as n decreases. More surprising, the exponent α_c remains pinned[79, 80] at 2 for the $U \rightarrow \infty$ limit of the Hubbard model at any filling. In fact, at any value of U , $\alpha_c = 2$ [79, 80] in the dilute regime of the Hubbard model in $d = 1$. In the $t - J$ model[79] ($t = J$), α_c starts at 2 at $n = 1$ and approaches a value of 4 at $n = 0$. Note, $\alpha_c = 4$ is the non-interacting value. That is, in $d = 1$ in the dilute regime, density correlations decay as r^{-2} in the $U \rightarrow \infty$ Hubbard model and as r^{-4} in the $t - J$ ($t=J$). This discrepancy is a clear indicator that relevant low-energy physics is lost if double occupancy of bare electrons is projected out in the parameter range considered here. Supposedly, this is captured by the t/U corrections to the electron operators in Eq. (16). In the procedure we outline in the Section III, we show that all of the physics described by the string of operators in the t/U corrections (Eq. (16) is described by a single charge $2e$ bosonic field.

3. New Theory: Hidden Charge $2e$ Boson

The Wilsonian program for constructing a low-energy theory is to explicitly integrate over the fields at high energy. The theory that results from this procedure should contain all the physics at low energy. In the context of the Hubbard model, it should explicitly tell us that $L/n_h > 1$, a key defining feature of a gapped phase without symmetry breaking. We now show how this comes about.

For the Hubbard model, one has to cleanly associate the physics on the energy scale U with an elemental field that can be integrated out either by using fermionic or bosonic path-integral methods. The Hubbard model in its traditional form does not admit such a treatment. However, one can bring the Hubbard model into the

Table 1. Comparison between Hubbard and t-J models. The exponents α_c and θ were computed using Bethe ansatz for the supersymmetric ($t = J$) t - J and Hubbard models in $d = 1$. Respectively, these exponents govern the asymptotic form of the density correlations and the momentum distribution functions. Z_{1h} denotes the quasiparticle weight for a single hole in Mott insulator described by either the Hubbard or t-J models, $\sigma(T = 0, n > 0.9)$ the conductivity for fillings exceeding $n = 0.9$, and Mid-IR denotes the mid-infrared band in the optical conductivity

	t - J	Hubbard
$\alpha_c(n = 0)$	4[79]	2[80]
θ	$(\alpha_c - 4)^2/16\alpha_c$ [79]	$1/8 \quad U \rightarrow \infty$ [80]
Z_{1h}	finite[72, 73, 74]	$L^{-\alpha}$ [75]
Mid-IR	none[82, 83]	yes[84, 85]
Luttinger surface at $n=1$	none[86, 87, 89]	yes[87, 59, 89]

appropriate form by introducing an elemental field that describes the excitations far away from the chemical potential. For hole-doping, this constitutes the excitations in the upper-Hubbard band. In our construction, we will extend the Hilbert space of the Hubbard model to include an extra degree of freedom which will represent the upper Hubbard band. By a constraint, the new field will represent the creation of double occupancy. This field will enter the Lagrangian with a mass of U . When the constraint is solved, we recover the Hubbard model. However, since the new field has a mass of U , the exact low-energy theory is obtained by integrating over this field rather than by solving the constraint. Consequently, the new low-energy theory will contain an extra degree of freedom having to do with the coupling with the high energy scale. Since the constraint field has to do with double occupancy, it must have charge $2e$.

3.1. Bohm/Pines Redux

There is a great similarity between our treatment of the new collective mode in the Hubbard model and the Bohm-Pines derivation of plasmons. Here we briefly introduce the approach used by Bohm and Pines[90] to describe the collective excitation of the interacting electron gas. Shankar and Murthy[91] also used a similar approach in their dipole analysis of the $\nu = 1/2$ quantum Hall state. The basic idea is to re-express the Hamiltonian in such a way that the long-range part of the Coulomb interactions between the electron is described in terms of collective fields (plasma mode) by enlarging the original Hilbert space. After we remove the unphysical states by a constraint, the resultant Hamiltonian will transform to an interacting electron gas with only short-range Coulomb interactions coupled to a plasma oscillating mode.

The starting point is the general interacting electron Hamiltonian,

$$H = \sum_i \frac{p_i^2}{2m} + 2\pi e^2 \sum_{kij} \frac{e^{i\mathbf{k}\cdot(\mathbf{x}_i - \mathbf{x}_j)}}{k^2} - 2\pi n e^2 \sum_k \frac{1}{k^2}$$

where n is the total electron density, the first term corresponds to the kinetic energy of

the electrons, the second term is their Coulomb interaction and the third term is the self-energy which represents a uniform positive charge background.

The collective mode can be described by first enlarging the Hilbert space of the original electron gas to include a new set of canonical variables, (π_k, θ_k) such that $[\theta_k, \pi_{k'}] = i\hbar\delta_{k,k'}$. The original Hamiltonian becomes,

$$\begin{aligned} H = & \sum_i \frac{p_i^2}{2m} - 2\pi n e^2 \sum_k \left(\frac{1}{k^2} \right) \\ & + \frac{\sqrt{4\pi}e}{m} \sum_{ik} \epsilon_k \cdot (\mathbf{p}_i - \hbar\mathbf{k}/2) \theta_k e^{i\mathbf{k}\cdot\mathbf{x}_i} - \sum_k \frac{1}{2} \pi_k \pi_{-k} \\ & + \frac{2\pi e^2}{m} \sum_{ikl} \epsilon_k \cdot \epsilon_l \theta_k \theta_l e^{i(\mathbf{k}+\mathbf{l})\cdot\mathbf{x}_i} \end{aligned} \quad (20)$$

Here, ϵ_k is the unit vector along the \mathbf{k} direction. The relevant equation can be derived by rewriting the Hamiltonian as a non-interacting electron system coupled to an external electric field, $\mathbf{E}(\mathbf{x})$,

$$H = \sum_i \frac{1}{2m} \left(p_i - \frac{e}{c} A_i(\mathbf{x}) \right)^2 + \frac{1}{8\pi} \mathbf{E}(\mathbf{x})^2, \quad (21)$$

such that

$$\mathbf{E}(\mathbf{x}) = \sqrt{4\pi} \sum_k \pi_{-k} \epsilon_k e^{i\mathbf{k}\cdot\mathbf{x}}. \quad (22)$$

The corresponding longitudinal vector potential $\mathbf{A}(\mathbf{x})$ is

$$\mathbf{A}(\mathbf{x}) = \sqrt{4\pi c^2} \sum_k \theta_k \epsilon_k e^{i\mathbf{k}\cdot\mathbf{x}}. \quad (23)$$

Here, both $\mathbf{A}(\mathbf{x})$ and $\mathbf{E}(\mathbf{x})$ are real and the unphysical states can be removed by the constraint,

$$\Omega_k = \pi_k - i \left(\frac{4\pi e^2}{k^2} \right)^{\frac{1}{2}} \sum_i e^{-i\mathbf{k}\cdot\mathbf{x}_i} = 0 \quad \forall \mathbf{k}, \quad (24)$$

which was obtained by equating the electric field energy, $\mathbf{E}(\mathbf{x})^2/8\pi$ with the electron-electron interaction energy. For the last term in Eq. (20), the dominant part comes from $\mathbf{k} = -\mathbf{l}$. By defining the plasma frequency

$$\omega_p^2 = \frac{4\pi n e^2}{m}, \quad (25)$$

we are able to simplify the Hamiltonian

$$\begin{aligned} H = & \sum_i \frac{p_i^2}{2m} - 2\pi n e^2 \sum_k \left(\frac{1}{k^2} \right) + \frac{\sqrt{4\pi}e}{m} \sum_{ik} \epsilon_k \cdot (\mathbf{p}_i - \hbar\mathbf{k}/2) \theta_k e^{i\mathbf{k}\cdot\mathbf{x}_i} \\ & - \frac{1}{2} \sum_k \left(\pi_k \pi_{-k} + \omega_p^2 \theta_k \theta_{-k} \right), \end{aligned} \quad (26)$$

which describes the non-interacting electron gas coupled with the plasma mode of frequency ω_p . Here, we have simplified the derivation by assuming the collective modes can oscillate with any frequency. In a realistic system, a maximum cutoff frequency,

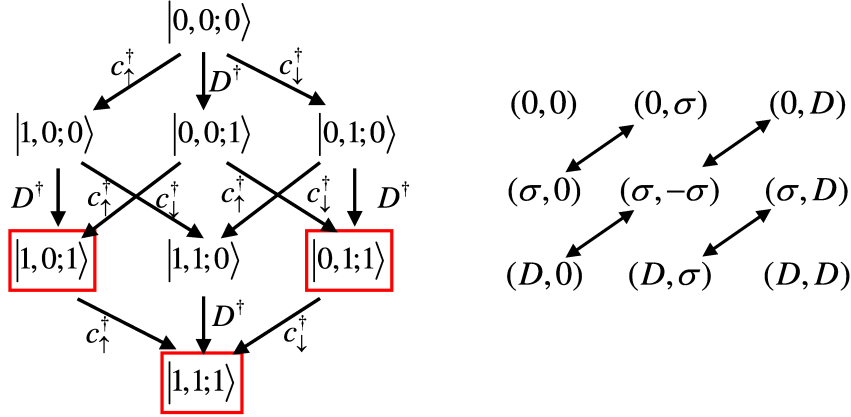


Figure 7. a) Extended Hilbert space which allows a clean coarse-graining on the energy scale U . b) Hopping processes which are included in the Lagrangian in the extended Hilbert space.

k_c , determined by the electron density, arises so that only the long-range electron-electron interaction can be transformed into the plasma mode, and the electron gas retains a short-range Coulomb interaction. The magnitude of k_c can be determined self-consistently by minimizing the total energy. To summarize, we have mapped the original electron-electron interacting Hamiltonian to a non-interacting electron gas coupled to the plasma mode. The key trick that made this happen was enlarging the original Hilbert space.

3.2. Charge $2e$ Boson

The essence of the Bohm-Pines[90] derivation is that plasmons, as an independent degree of freedom, are only apparent when the constraint is relaxed in the extended Hilbert space. As we will see, the same is true for a doped Mott insulator. To this end[9, 10], we extend the Hilbert space $\otimes_i (\mathcal{F}_{\uparrow} \otimes \mathcal{F}_{\downarrow} \otimes \mathcal{F}_D)$, where \mathcal{F} denotes a fermionic Fock space. In the left frame of Fig. (7), we indicate the states of the extended Hilbert space for a single site. The new extended states are shown in red. Such states will be removed by a suitably chosen constraint which will associate D_i^{\dagger} with the creation of double-occupation. In order to limit the Hilbert space to single occupation in the D sector, we will take D to be fermionic. The field D will enter the theory as an elemental field with a large (order U) quadratic term and precise interactions with the electronic degrees of freedom; the low-energy (IR) theory is obtained by integrating out D . Because D is fermionic, a trick is required to associate it with the creation of double occupancy which clearly transforms as a boson. Essentially, we will have to fermionize double occupancy. This can be done by imposing a constraint on the D_i field such that

$$D_i \approx \theta c_{i\uparrow} c_{i\downarrow} \quad (27)$$

where θ is a Grassmann field which is normalized as

$$\int d^2\theta \bar{\theta}\theta = 1. \quad (28)$$

The constraint will be imposed through the use of a δ -function and hence will enter the action upon a subsequent exponentiation as in the implementation of the constraint in the non-linear σ -model. While there is some similarity between θ and a super-coordinate, this association is strictly formal in our case as any dependence on the Grassmann parameter θ disappears.

For hole-doping, it is the upper Hubbard band that must be integrated out. The appropriate hopping processes that must be included in the Lagrangian are given in the right-hand panel of Fig. (7). The Euclidean Lagrangian in the extended Hilbert space which describes the hopping processes detailed above can be written

$$\begin{aligned} \mathcal{L} = \int d^2\theta \left[\bar{\theta}\theta \sum_{i,\sigma} (1 - n_{i,-\sigma}) c_{i,\sigma}^\dagger \dot{c}_{i,\sigma} + \sum_i D_i^\dagger \dot{D}_i \right. \\ \left. + U \sum_j D_j^\dagger D_j - t \sum_{i,j,\sigma} g_{ij} \left[C_{ij,\sigma} c_{i,\sigma}^\dagger c_{j,\sigma} + D_i^\dagger c_{j,\sigma}^\dagger c_{i,\sigma} D_j \right. \right. \\ \left. \left. + (D_j^\dagger \theta c_{i,\sigma} V_\sigma c_{j,-\sigma} + h.c.) \right] + H_{\text{con}} \right]. \quad (29) \end{aligned}$$

Here, g_{ij} selects out nearest neighbours (note that if we wanted to include next-to-nearest neighbour interactions, we need just modify the matrix g_{ij} accordingly), the parameter V_σ has values $V_\uparrow = 1$, $V_\downarrow = -1$, and simply ensures that D couples to the spin singlet and the operator $C_{ij,\sigma}$ is of the form $C_{ij,\sigma} \equiv \bar{\theta}\theta \alpha_{ij,\sigma} \equiv \bar{\theta}\theta (1 - n_{i,-\sigma})(1 - n_{j,-\sigma})$ with number operators $n_{i,\sigma} \equiv c_{i,\sigma}^\dagger c_{i,\sigma}$. Note that the dynamical terms that appear in the Lagrangian exclude, as they must, those sites already singly occupied, as they describe the dynamics in the LHB. The constraint Hamiltonian H_{con} is taken to be

$$H_{\text{con}} = s\bar{\theta} \sum_j \varphi_j^\dagger (D_j - \theta c_{j,\uparrow} c_{j,\downarrow}) + h.c., \quad (30)$$

where φ is a complex charge $2e$ bosonic field which enters the theory as a Lagrange multiplier. The constant s has been inserted to carry the units of energy. It could be absorbed into the definition of the constraint field φ . There is a natural connection between φ_i in our theory and σ in the non-linear σ -model. Both start their lives as Lagrange multipliers but both end up affecting the low-energy physics. At this point, there is some ambiguity in the normalization of φ , but we expect that this will be set dynamically. We will find that if a true infrared limit exists, then s must be of order the hopping matrix element t .

Now, as remarked previously, we have chosen the Lagrangian (29) so that this theory is equivalent to the Hubbard model. To demonstrate this, we first show that once the constraint is solved, we obtain the Hubbard model. Hence, the Lagrangian we have formulated is the Hubbard model written in a non-traditional form – in a sense, we have inserted unity into the Hubbard model path integral in a rather complicated fashion. To this end, we compute the partition function

$$Z = \int [\mathcal{D}c \mathcal{D}c^\dagger \mathcal{D}D \mathcal{D}D^\dagger \mathcal{D}\varphi \mathcal{D}\varphi^\dagger] \exp^{-\int_0^\tau \mathcal{L} dt}. \quad (31)$$

with \mathcal{L} given by (29). We note that φ is a Lagrange multiplier. As shown previously[10], in the Euclidean signature, the fluctuations of the real and imaginary parts of φ_i must be integrated along the imaginary axis for φ_i to be regarded as a Lagrangian multiplier. The φ integrations (over the real and imaginary parts) are precisely a representation of (a series of) δ -functions of the form,

$$\delta\left(\int d\theta D_i - \int d\theta \theta c_{i,\uparrow} c_{i,\downarrow}\right). \quad (32)$$

If we wish to recover the Hubbard model, we need only to integrate over D_i , which is straightforward because of the δ -functions. The dynamical terms yield

$$\begin{aligned} & \int d^2\theta \bar{\theta}\theta \left[\sum_{i,\sigma} (1 - n_{i,-\sigma}) c_{i,\sigma}^\dagger \dot{c}_{i,\sigma} + \sum_i c_{i,\downarrow}^\dagger c_{i,\uparrow}^\dagger \dot{c}_{i,\uparrow} c_{i,\downarrow} \right. \\ & \quad \left. + \sum_i c_{i,\downarrow}^\dagger c_{i,\uparrow}^\dagger c_{i,\uparrow} \dot{c}_{i,\downarrow} \right] \\ &= \int d^2\theta \bar{\theta}\theta \sum_{i,\sigma} \left[(1 - n_{i,-\sigma}) c_{i,\sigma}^\dagger \dot{c}_{i,\sigma} + n_{i,-\sigma} c_{i,\sigma}^\dagger \dot{c}_{i,\sigma} \right] \\ &= \int d^2\theta \bar{\theta}\theta \sum_{i,\sigma} c_{i,\sigma}^\dagger \dot{c}_{i,\sigma}. \end{aligned} \quad (33)$$

Likewise the term proportional to V_σ yields

$$\begin{aligned} & \int d^2\theta \bar{\theta}\theta \sum_{i,j} g_{ij} \left[c_{j,\downarrow}^\dagger c_{j,\uparrow}^\dagger (c_{i,\uparrow} c_{j,\downarrow} - c_{i,\downarrow} c_{j,\uparrow}) \right] + h.c. \\ &= \int d^2\theta \bar{\theta}\theta \sum_{i,j,\sigma} g_{ij} n_{j,-\sigma} c_{j,\sigma}^\dagger c_{i,\sigma} + h.c. \end{aligned} \quad (34)$$

Finally, the two D field terms give rise to

$$\begin{aligned} & \int d^2\theta \bar{\theta}\theta \sum_{i,j} g_{ij} \left[c_{i,\downarrow}^\dagger c_{i,\uparrow}^\dagger (c_{j,\uparrow}^\dagger c_{i,\uparrow} + c_{j,\downarrow}^\dagger c_{i,\downarrow}) c_{j,\uparrow} c_{j,\downarrow} \right] \\ &= - \int d^2\theta \bar{\theta}\theta \sum_{i,j} g_{ij} n_{j,-\sigma} n_{i,-\sigma} c_{i,\sigma}^\dagger c_{j,\sigma}. \end{aligned} \quad (35)$$

Eqs. (34) and (35) add to the constrained hopping term in the Lagrangian (the term proportional to $C_{ij,\sigma}$) to yield the standard kinetic energy term in the Hubbard model. Finally, the $D^\dagger D$ term generates the on-site repulsion of the Hubbard model. Consequently, by integrating over φ_i followed by an integration over D_i , we recover the Lagrangian,

$$\int d^2\theta \bar{\theta}\theta \mathcal{L}_{\text{Hubb}} = \sum_{i,\sigma} c_{i,\sigma}^\dagger \dot{c}_{i,\sigma} + H_{\text{Hubb}}, \quad (36)$$

of the Hubbard model. This constitutes the ultra-violet (UV) limit of our theory. In this limit, it is clear that the Grassmann variables amount to an insertion of unity and hence play no role. Further, in this limit the extended Hilbert space contracts, unphysical states such as $|1, 0, 1\rangle$, $|0, 1, 1\rangle$, $|1, 1, 1\rangle$ are set to zero, and we identify $|1, 1, 0\rangle$ with $|0, 0, 1\rangle$. Note there is no contradiction between treating D as fermionic and the constraint in Eq. (30). The constraint never governs the commutation relation for D .

The value of D is determined by Eq. (30) only when φ is integrated over. This is followed immediately by an integration over D at which point D is eliminated from the theory.

The advantage of our starting Lagrangian over the traditional writing of the Hubbard model is that we are able to coarse grain the system cleanly for $U \gg t$. The energy scale associated with D is the large on-site energy U . Hence, it makes sense, instead of solving the constraint, to integrate out D . The resultant theory will contain explicitly the bosonic field, φ . As a result of this field, double occupancy will remain, though the energy cost will be shifted from the UV to the infrared (IR). Because the theory is Gaussian, the integration over D_i can be done exactly. This is the ultimate utility of the expansion of the Hilbert space – we have isolated the high energy physics into this Gaussian field. As a result of the dynamical term in the action, integration over D will yield a theory that is frequency dependent. The frequency will enter in the combination $\omega + U$ which will appear in denominators. Since U is the largest energy scale, we expand in powers of ω/U ; the leading term yields the proper $\omega = 0$ low-energy theory. Since the theory is Gaussian, it suffices to complete the square in the D -field. To accomplish this, we define the matrix

$$\mathcal{M}_{ij} = \delta_{ij} - \frac{t}{(\omega + U)} g_{ij} \sum_{\sigma} c_{j,\sigma}^{\dagger} c_{i,\sigma} \quad (37)$$

and $b_i = \sum_j b_{ij} = \sum_{j,\sigma} g_{ij} c_{j,\sigma} V_{\sigma} c_{i,-\sigma}$. At zero frequency the Hamiltonian is

$$H_h^{IR} = -t \sum_{i,j,\sigma} g_{ij} \alpha_{ij,\sigma} c_{i,\sigma}^{\dagger} c_{j,\sigma} + H_{\text{int}} - \frac{1}{\beta} \text{Tr} \ln \mathcal{M},$$

where

$$\begin{aligned} H_{\text{int}} = & -\frac{t^2}{U} \sum_{j,k} b_j^{\dagger} (\mathcal{M}^{-1})_{jk} b_k - \frac{s^2}{U} \sum_{i,j} \varphi_i^{\dagger} (\mathcal{M}^{-1})_{ij} \varphi_j \\ & - s \sum_j \varphi_j^{\dagger} c_{j,\uparrow} c_{j,\downarrow} + \frac{st}{U} \sum_{i,j} \varphi_i^{\dagger} (\mathcal{M}^{-1})_{ij} b_j + h.c. \end{aligned} \quad (38)$$

which constitutes the true (IR) limit as long as the energy scale s is not of order U . As we have retained all powers of t/U , Eq. (38) is exact. If $s \sim O(U)$ then we should also integrate out φ_i – this integration is again Gaussian and can be done exactly; one can easily check that this leads precisely back to the UV theory, the Hubbard model. Hence, the only way in which a low-energy theory of the Hubbard model exists is if the energy scale for the dynamics that φ mediates is $O(t)$. This observation is significant because it lays plain the principal condition for the existence of an IR limit of the Hubbard model. Since the order of integrations we have performed here does not matter, integration over φ_i in the path integral for the action corresponding to Eq. (38) also yields the Hubbard model. As we have shown elsewhere[10] the Wick rotation must be taken into consideration to complete the Gaussian integration over φ_i . Finally, as we have shown previously[10], the theory derived here could easily have been constructed in terms of the Hubbard operators, ξ and η . This offers no further complication. In so doing, the spin-spin interaction which arises from the first term in Eq. (38) would have

been projected onto a subspace which prohibits double occupancy. That is, it would be equivalent to the spin-spin interaction in the standard $t - J$ model. Since double occupancy still survives at low energies and is mediated by the φ_i terms, such a rewriting of the low-energy Hamiltonian is strictly optional.

To fix the constant s , we determine how the electron operator transforms in the exact theory. As is standard, we add a source term to the starting Lagrangian which generates the canonical electron operator when the constraint is solved. For hole-doping, the appropriate transformation that yields the canonical electron operator in the UV is

$$\mathcal{L} \rightarrow \mathcal{L} + \sum_{i,\sigma} J_{i,\sigma} \left[\bar{\theta}\theta(1 - n_{i,-\sigma})c_{i,\sigma}^\dagger + V_\sigma D_i^\dagger \theta c_{i,-\sigma} \right] + h.c.$$

However, in the IR in which we only integrate over the heavy degree of freedom, D_i , the electron creation operator becomes

$$c_{i,\sigma}^\dagger \rightarrow (1 - n_{i,-\sigma})c_{i,\sigma}^\dagger + V_\sigma \frac{t}{U} b_i c_{i,-\sigma} + V_\sigma \frac{s}{U} \varphi_i^\dagger c_{i,-\sigma} \quad (39)$$

to linear order in t/U . This equation resembles the transformed electron operator in Eq. (16). In fact, the first two terms are identical. The last term in Eq. (16) is associated with double occupation. In Eq. (39), this role is played by φ_i . Demanding that Eqs. (16) and (39) agree requires that $s = t$, thereby eliminating any ambiguity associated with the constraint field. Consequently, the complicated interactions appearing in Eq. (16) as a result of the inequivalence between $c_{i\sigma}$ and $f_{i\sigma}$ are replaced by a single charge $2e$ bosonic field φ_i which generates dynamical spectral weight transfer across the Mott gap. The interaction in Fig. (5), corresponding to the second-order process in the term $\varphi_i^\dagger b_i$, is the key physical process that enters the dynamics at low-energy. That the dynamical spectral weight transfer can be captured by a charge $2e$ bosonic degree of freedom is the key outcome of the exact integration of the high-energy scale. This bosonic field represents a collective excitation of the upper and lower Hubbard bands. Hence, we have successfully unearthed the extra degree of freedom associated with $L/n_h > 1$ physics in a doped Mott insulator.

3.3. Half-Filling: Mott gap and antiferromagnetism

There is an important simplification that obtains at half-filling that points to one of the potential uses of this theory: the dynamical mode that generates the Mott gap. Recall our ultimate task was to integrate out the degrees of freedom far away from the chemical potential. At half-filling, both the lower and upper Hubbard bands are at high energy. Hence, both must be integrated out to obtain the true low-energy theory. However, at present, we have only integrated out the UHB. Because the integration of the UHB is not equivalent to simply integrating out double occupancy, a trivial particle-hole transformation does not help us to determine how the low-energy theory should be formulated in this case.

Ultimately we have to introduce two new fermionic fields D and \tilde{D} associated with the double occupancy and double holes, respectively. To proceed, we consider the

Lagrangian,

$$\begin{aligned} \mathcal{L}_{\text{UV}}^{\text{hf}} = & \int d^2\theta \left[iD^\dagger \dot{D} + i\tilde{D}\dot{\tilde{D}}^\dagger - \frac{U}{2}(D^\dagger D - \tilde{D}\tilde{D}^\dagger) \right. \\ & + \frac{t}{2}D^\dagger \theta b + \frac{t}{2}\bar{\theta} b \tilde{D} + h.c. + s\bar{\theta}\varphi^\dagger(D - \theta c_\uparrow c_\downarrow) \\ & \left. + \tilde{s}\bar{\theta}\tilde{\varphi}^\dagger(\tilde{D} - \theta c_\uparrow^\dagger c_\downarrow^\dagger) + h.c. \right], \end{aligned} \quad (40)$$

contains the two constraint charge $\pm 2e$ bosonic fields, φ_i^\dagger (charge $2e$) and $\tilde{\varphi}_i^\dagger$ (charge $-2e$) which enter the theory as Lagrange multipliers for the creation of double occupancy and double holes, respectively. Similar to the previous result, if we first integrate out both the bosonic fields φ_i , $\tilde{\varphi}_i$ and then D_i , \tilde{D}_i , the Hubbard model is obtained and the generalised theory Eq.40 yields the correct UV limit. In deriving the UV limit, it is crucial that the operators representing the creation of double occupancy and double holes remain in the order indicated in the Lagrangian. However, a different IR limit is obtained if we first integrate out D_i and \tilde{D}_i ,

$$\begin{aligned} \mathcal{L}_{\text{IR}}^{\text{hf}} = & - \left(s\varphi^\dagger + \frac{1}{2}tb^\dagger \right) L_-^{-1} \left(s^*\varphi + \frac{1}{2}tb \right) \\ & + \left(\tilde{s}^*\tilde{\varphi} + \frac{1}{2}tb^\dagger \right) L_+^{-1} \left(\tilde{s}\tilde{\varphi}^\dagger + \frac{1}{2}tb \right) \\ & - \left(s\varphi^\dagger - \tilde{s}^*\tilde{\varphi} \right) c_\uparrow c_\downarrow + h.c., \end{aligned} \quad (41)$$

where $L_\pm = i\frac{d}{dt} \pm \frac{U}{2}$. This theory is exact and hence should contain the source of the Mott gap. This Lagrangian is invariant under the transformation $c_{i,\sigma} \rightarrow \exp(i\mathbf{Q}\cdot\mathbf{R}_i)c_{i,\sigma}^\dagger$, $\varphi_i \leftrightarrow \tilde{\varphi}_i$ and $s \leftrightarrow \tilde{s}$. This invariance reflects the symmetry between the double occupancy and the double hole in the system at half filling. In contrast to the doped case as in Eq. (38), no \mathcal{M} matrices appear in the IR theory at half filling. Consequently, we arrive at a closed form for the low-energy theory at half-filling in which no bare field has dynamics. The $b^\dagger b + bb^\dagger$ terms include a spin-spin interaction as well as a three-site hopping term. However, at half-filling, the three-site hopping term vanishes.

It is interesting to note that Eq. (41), as an exact low-energy theory of the Hubbard model, is not equivalent to the Heisenberg model. Only the $b^\dagger b$ terms yield the Heisenberg model. Hence, we consider the separation,

$$\mathcal{L}_{\text{Mott}} = \mathcal{L}_{\text{hf}}^{\text{IR}} + \frac{1}{4}t^2 b^\dagger L_-^{-1} b + \frac{1}{4}t^2 b^\dagger L_+^{-1} b \quad (42)$$

which explicitly removes the spin-spin term from the low-energy Lagrangian. As will be seen, the dynamics leading to the Mott gap can be constructed entirely from $\mathcal{L}_{\text{Mott}}$. That $\mathcal{L}_{\text{hf}}^{\text{IR}}$ is not equivalent to the Heisenberg model is not surprising for three related reasons. First, explicit evaluation of the path integral over the new degrees of freedom must regenerate the original Hubbard model. Hence, there must be something left over once we subtract the Heisenberg terms from the low-energy theory of the Hubbard model. Second, as pointed out previously[70, 71], the Heisenberg model has a local SU(2) symmetry not the global SU(2) symmetry of the Hubbard model. Hence, the true low-energy theory of the Hubbard model at half-filling must have other terms that

break the local SU(2) and reinstate the global SU(2) symmetry. As we have shown previously[10], all of the terms involving the φ_i and $\tilde{\varphi}_i$ degrees of freedom restore the global SU(2) symmetry. Consequently, the emergence of the new local SU(2) symmetry is a function entirely of projection onto the singly-occupied electron subspace. Third, at half-filling, the Hubbard model possesses a surface of zeros[86, 87] of the single-particle Green function along a connected surface in momentum space, whereas the Heisenberg model does not. The absence of such a surface of zeros, the Luttinger surface, is also a function of projection. In fact, all of these three failures of the Heisenberg model arise from hard projection, which Eq. (16) shows is not correct even at half-filling. The non-trivial implication of the zero surface is that the real part of the Green function,

$$R_\sigma(\mathbf{k}, 0) = - \int_{-\infty}^{-\Delta^-} d\epsilon' \frac{A_\sigma(\mathbf{k}, \epsilon')}{\epsilon'} - \int_{\Delta^+}^{\infty} d\epsilon' \frac{A_\sigma(\mathbf{k}, \epsilon')}{\epsilon'} \quad (43)$$

vanishes. Here $A_\sigma(k, \epsilon)$ is the single-particle spectral function which we are assuming to have a gap of width 2Δ symmetrically located about the chemical potential at $\epsilon = 0$. Because $A(\mathbf{k}, \epsilon) > 0$ away from the gap, and ϵ changes sign above and below the gap, Eq. (43) can pass through zero. For this state of affairs to obtain, the pieces of the integral below and above the gap must be retained. Projected models which throw away the UHB fail to recover the zero surface.

3.3.1. Mott Gap What Eq. (41) makes clear is that all the information regarding the surface of zeros is now encoded into the bosonic fields φ_i and $\tilde{\varphi}_i$. While numerical methods[92, 93] exist which lead to a Mott gap, there has been no explicit demonstration of the dynamical degrees of freedom that ultimately generate this gap. The bosonic degrees of freedom in Eq. (41) solve this problem.

To proceed, we transform to frequency and momentum space and focus on a square lattice as in the cuprates. Defining $\varphi(t) = \int d\omega e^{-i\omega t} \varphi_\omega$, the energy dispersion, $\varepsilon_{\mathbf{p}}^{(\mathbf{k})} = 4 \sum_\mu \cos(k_\mu a/2) \cos(p_\mu a)$, and the Fourier transform of b_i ,

$$b_{\mathbf{k}} = \sum_{\mathbf{p}} \varepsilon_{\mathbf{p}}^{(\mathbf{k})} c_{\mathbf{k}/2+\mathbf{p},\uparrow} c_{\mathbf{k}/2-\mathbf{p},\downarrow}, \quad (44)$$

we arrive at the exact working expression,

$$\begin{aligned} \mathcal{L}_{\text{IR}}^{\text{hf}} = & - \frac{|s|^2}{(\omega - U/2)} \varphi_{\omega,\mathbf{k}}^\dagger \varphi_{\omega,\mathbf{k}} + \frac{|s|^2}{(\omega + U/2)} \tilde{\varphi}_{-\omega,\mathbf{k}}^\dagger \tilde{\varphi}_{-\omega,\mathbf{k}} \\ & + \frac{Ut^2}{U^2 - 4\omega^2} b_{\omega,\mathbf{k}}^\dagger b_{\omega,\mathbf{k}} \\ & + (s\alpha_{\mathbf{p}}^{(\mathbf{k})}(\omega) \varphi_{\omega,\mathbf{k}}^\dagger + \tilde{s}^* \tilde{\alpha}_{\mathbf{p}}^{(\mathbf{k})}(\omega) \tilde{\varphi}_{-\omega,\mathbf{k}}) \\ & \times (c_{\mathbf{k}/2+\mathbf{p},\uparrow} c_{\mathbf{k}/2-\mathbf{p},\downarrow})_\omega + h.c. \end{aligned} \quad (45)$$

for the low-energy Lagrangian where we have suppressed the implied integration over frequency and introduced the coupling constants,

$$\begin{aligned} \alpha_{\mathbf{p}}^{(\mathbf{k})}(\omega) &= \frac{U - t\varepsilon_{\mathbf{p}}^{(\mathbf{k})} - 2\omega}{U - 2\omega} \\ \tilde{\alpha}_{\mathbf{p}}^{(\mathbf{k})}(\omega) &= \frac{U + t\varepsilon_{\mathbf{p}}^{(\mathbf{k})} + 2\omega}{U + 2\omega} \end{aligned} \quad (46)$$

which play a central role in this theory. They, in fact, will determine the spectral weight in the lower and upper Hubbard bands, respectively.

Although Eq. (45) lacks any kinetic terms, an analysis similar to that used by Polchinski[42] in the context of Fermi liquids can be used. The key point in that argument is that all renormalizations are towards the surface in momentum space where the spectral weight resides. In a theory of weakly coupled constituents, setting the coefficient of the quadratic terms in a Lagrangian would determine their dispersion. As is evident from Eq. (45), the coupling constants for all of the quadratic terms never vanish. All else being equal, this implies that there is no spectral weight anywhere. What we have shown[95] is that the terms in which the bosonic degrees of freedom and the fermions are coupled determine where spectral weight resides. In fact, it is these terms that should properly be regarded as quadratic. To this end, we make the transformation, $\varphi_\omega \rightarrow \sqrt{1 - 2\omega/U} \varphi_\omega$, $\tilde{\varphi}_\omega \rightarrow \sqrt{1 + 2\omega/U} \tilde{\varphi}_\omega$, and $(cc)_\omega \rightarrow \sqrt{1 - 4\omega^2/U^2} (cc)_\omega$ which recasts the Lagrangian as

$$L_{\text{IR}}^{\text{hf}} \rightarrow 2 \frac{|s|^2}{U} |\varphi_\omega|^2 + 2 \frac{|\tilde{s}|^2}{U} |\tilde{\varphi}_{-\omega}|^2 + \frac{t^2}{U} |b_\omega|^2 \quad (47)$$

$$+ s \gamma_{\mathbf{p}}^{(\mathbf{k})}(\omega) \varphi_{\omega, \mathbf{k}}^\dagger c_{\mathbf{k}/2 + \mathbf{p}, \omega/2 + \omega', \uparrow} c_{\mathbf{k}/2 - \mathbf{p}, \omega/2 - \omega', \downarrow} \quad (48)$$

$$+ \tilde{s}^* \tilde{\gamma}_{\mathbf{p}}^{(\mathbf{k})}(\omega) \tilde{\varphi}_{-\omega, \mathbf{k}} c_{\mathbf{k}/2 + \mathbf{p}, \omega/2 + \omega', \uparrow} c_{\mathbf{k}/2 - \mathbf{p}, \omega/2 - \omega', \downarrow} \\ + h.c. \quad (49)$$

where

$$\gamma_{\mathbf{p}}^{(\mathbf{k})}(\omega) = \frac{-U + t\varepsilon_{\mathbf{p}}^{(\mathbf{k})} + 2\omega}{U} \sqrt{1 + 2\omega/U} \\ \tilde{\gamma}_{\mathbf{p}}^{(\mathbf{k})}(\omega) = \frac{U + t\varepsilon_{\mathbf{p}}^{(\mathbf{k})} + 2\omega}{U} \sqrt{1 - 2\omega/U}. \quad (50)$$

The vanishing of the coefficients $\gamma_{\mathbf{p}}^{\mathbf{k}}$ and $\tilde{\gamma}_{\mathbf{p}}^{\mathbf{k}}$ determine where the spectral weight lies. Consider initially $\mathbf{k} = 0$ so that the dispersion simplifies to $4 \sum_{\mu} \cos p_{\mu}$. When $\omega = U/2$ ($\omega = -U/2$), $\sum_{\mu} \cos p_{\mu} = 0$ defines the momentum surface along which $\gamma_{\mathbf{p}}$ ($\tilde{\gamma}_{\mathbf{p}}$) vanishes. This surface corresponds to the diamond $a\mathbf{p} = (ap_x, \pm\pi - ap_x)$ as depicted in Fig. (9). These features define the center of the LHB ($-U/2$) and UHB ($U/2$). At each momentum in the first Brillouin zone (FBZ), spectral weight develops at two distinct energies. This state of affairs obtains because $\gamma_{\mathbf{p}} = 0$ between $U/2 - 4t \leq \omega \leq U/2 + 4t$ and $\tilde{\gamma}_{\mathbf{p}} = 0$ for $-U/2 - 4t \leq \omega \leq -U/2 + 4t$ for each momentum state in the FBZ. Within each energy range, the associated operator, which is of the form $\varphi^\dagger cc$ (UHB) or $\tilde{\varphi} cc$ (LHB), can be viewed as a quadratic kinetic term. The $(0, 0)$ point corresponds to the lowest energy state in each LHB and UHB, that is, $\omega = -U/2 - 4t$ and $\omega = U/2 - 4t$ whereas (π, π) sits at the top of each band at $\omega = -U/2 + 4t$ and $\omega = U/2 + 4t$. Consequently, at each momentum, the splitting between the turn-on of the spectral weight in the UHB and LHB is U . When $U > W$, each momentum state lacks spectral weight over a common range of energies. As a consequence, a hard gap opens in the spectrum. This is the Mott gap (for the composite excitations not the electrons), and its origin is the emergence of composite excitations described by the operators $\varphi^\dagger cc$ (UHB) and $\tilde{\varphi} cc$

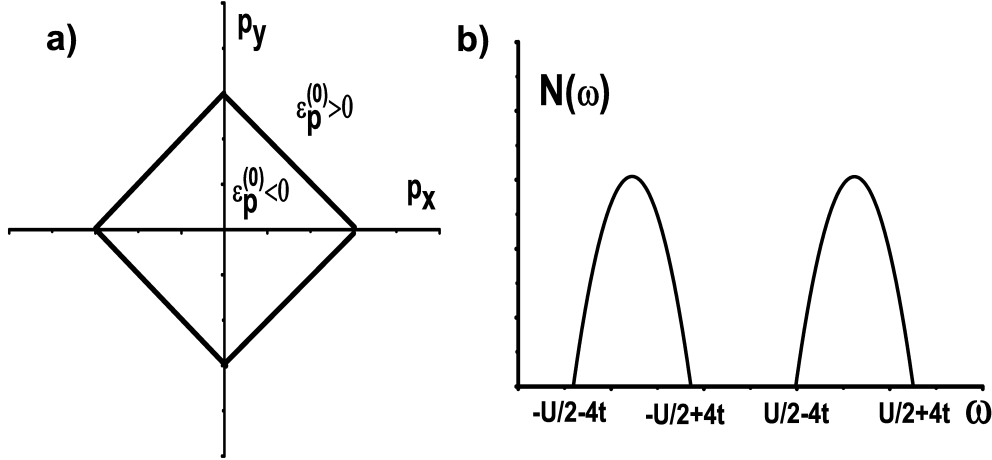


Figure 8. a) Diamond-shaped surface in momentum space where the particle dispersion changes sign. b) Turn-on of the spectral weight in the upper and lower Hubbard bands as a function of energy and momentum. In the UHB, the spectral density is determined to $\gamma_{\mathbf{p}}$ while for the LHB it is governed by $\tilde{\gamma}_{\mathbf{p}}$. The corresponding operators which describe the turn-on of the spectral weight are the composite excitations $\varphi^{\dagger}cc$ (UHB) and $\tilde{\varphi}cc$ (LHB).

(LHB), which we loosely interpret as bound states. As our analysis thus far is exact, we conclude that in the absence of any symmetry breaking, the coefficients $\gamma_{\mathbf{p}}$ and $\tilde{\gamma}_{\mathbf{p}}$ determine the dispersion for the excitations that comprise the here-to-fore undefined[47] UHB and LHB. Inclusion of the center-of-mass momentum \mathbf{k} simply shifts the value of the momentum at which the dispersion changes sign, thereby keeping the Mott gap in tact.

Thus far, we have established the Mott gap in terms of a set of composite excitations which are orthogonal in that they never lead to a turn-on of the spectral weight in the same range of energies. Ultimately, we would like to know the spectral function in terms of the original electron degrees of freedom. The lack of any derivative terms in the action with respect to φ_i implies that we can treat φ as a spatially homogeneous field. *A priori*, gradient terms with respect to φ_i are possible. However, such terms are absent from the exact low-energy theory as such terms would indicate the presence of a freely propagating bosonic degree of freedom at half-filling. It is precisely because such terms are absent that we were able to identify that the only propagating degrees of freedom at half-filling are gapped excitations.

To proceed, we rewrite the coefficient of the boson-fermi terms as

$$\Delta(k, \omega, \phi, \tilde{\phi}) = -s(\phi^{\dagger} - \tilde{\phi}) + \left(\frac{st}{U - 2\omega - i\delta} \phi^{\dagger} + \frac{st}{U + 2\omega + i\delta} \tilde{\phi} \right) \alpha(k)$$

and

$$\alpha(k) = 2t(\cos(k_x) + \cos(k_y)). \quad (51)$$

In this treatment, any non-trivial dynamics leading to the Mott gap will arise only from the the second term in $\Delta(k, \omega, \phi, \tilde{\phi})$. Performing the Wick rotation, $\phi \rightarrow i\phi$ and

$\phi^* \rightarrow i\phi^*$, we recast the single-particle electron Green function as

$$G(k, \omega) = \int d\phi \int d\tilde{\phi} G(k, \omega, \phi, \tilde{\phi}) \exp^{-\int d\omega \mathcal{L}_{\text{Mott}}} \quad (52)$$

where

$$G(k, \omega, \phi, \tilde{\phi}) = \frac{i\delta}{|\Delta(k, \omega, \phi, \tilde{\phi})|^2 + i\delta}. \quad (53)$$

At first glance, the Green function seems to have a vanishing imaginary part. However, because of the $i\delta$ in the gap function, $\Delta(k, \omega, \phi, \tilde{\phi})$, the imaginary part of the Green function

$$\begin{aligned} \Im G(k, \omega, \phi, \tilde{\phi}) &= \lim_{\delta \rightarrow 0} \left[(U - 2\omega)^2 + \delta^2 \right] \left[(U + 2\omega)^2 + \delta^2 \right] \\ &\quad \times \frac{\delta}{A^2 + (2A(\phi + \tilde{\phi}) + B^2) \delta^2 + O(\delta^4)} \\ &= \frac{(U - 2\omega)^2 (U + 2\omega)^2}{B} \delta(A) \end{aligned} \quad (54)$$

is explicitly non-zero. Here

$$\begin{aligned} A &= \left[U^2 - 4\omega^2 - 2\alpha_k(U + 2\omega) \right] \phi + \left[U^2 - 4\omega^2 - 2\alpha_k(U - 2\omega) \right] \tilde{\phi} \\ B &= 2\phi(2\omega + \alpha_k) + 2\tilde{\phi}(2\omega + \alpha_k) \end{aligned} \quad (55)$$

To complete the calculation, we performed the φ_i and $\tilde{\varphi}$ integrations numerically. The results in Fig. (9) clearly show that a Mott gap exists and the spectral weight is momentum dependent. At $(0, 0)$, the spectral weight lies predominantly in the LHB whereas at (π, π) it lies in the UHB. Consequently, the real part of the Green function must change sign on some momentum surface between these two limits. The location of the zero surface is the Fermi surface of the non-interacting system as it must be for the half-filled system with particle-hole symmetry. We find then that the Mott gap arises from the dynamics of the two charge $|2e|$ bosonic fields. This is the first time the Mott gap has been derived dynamically, in particular by a collective degree of freedom of the lower and upper Hubbard bands. Relative to the gap in the spectrum for the composite excitations that diagonalise the fermion-boson terms in Eq. (49), the gap in the electron spectrum is larger. This is not surprising as the bare electrons do not have unit overlap with the composite excitations. In addition, the momentum dependence of the spectral function is identical to that obtained by dynamical mean-field calculations[92] thereby lending credence to such cluster[94].

An open question that this analysis provokes is whether or not the turn-on of the spectral weight in a Mott insulator is governed by a fixed point. If so, then in analogy with the Fermi liquid analysis[42], all the interactions except those that govern the turn-on of the spectral weight should be irrelevant. That is, the $\varphi^\dagger cc$ and the $\tilde{\varphi} cc$ terms represent a natural theory. Indeed, the analysis presented above demonstrates that the spin-spin term has nothing to do with the turn-on of the spectral weight, as foreshadowed by Mott[1]. Namely, the gap in the spectrum at half-filling is independent of ordering. While a naive scaling analysis suggests that the spin-spin interaction is

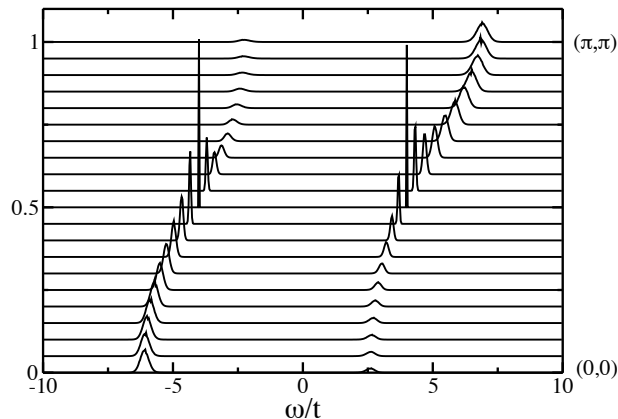


Figure 9. Electron spectral function corresponding to $\mathcal{L}_{\text{Mott}}$ for $U = 8t$. The gap here is generated entirely from the dynamics of the charge $2e$ bosonic fields that emerge from integrating out the upper and lower Hubbard bands at half-filling.

indeed subdominant, we have been unable to compute the β -function to show that a true fixed point underlies the physics at half-filling. Such a computation stands as a true challenge for Mottness.

Nonetheless, antiferromagnetism with an ordering wave-vector of (π, π) can also be understood within this formalism. Within this theory, there is a natural candidate for the antiferromagnetic order parameter, namely $B_{ij} = \langle g_{ij} \varphi_i^\dagger c_{i,\uparrow} c_{j,\downarrow} \rangle$. The vacuum expectation value of this quantity is clearly non-zero as it is easily obtained from a functional derivative of the partition function with respect to $\gamma_{\mathbf{p}}$. That this is the relevant order parameter instead of the traditional one follows from the fact that the spin-spin interaction and all higher-order operators contained in $|b|^2$ are at least proportional to a^4 (a the lattice constant) and hence are subdominant to the composite terms. Hence, a non-traditional order parameter must govern the turn-on of antiferromagnetism. We advocate that B_{ij} characterizes the antiferromagnet that describes the strong-coupling limit of the Hubbard model and as a consequence the insulating state of the cuprates. An antiferromagnet of this kind has no continuity with the antiferromagnet at weak coupling because it is mediated by the collective mode φ or $\tilde{\varphi}$. Hence, both the Mott gap and subsequent antiferromagnetic order emerge from composite excitations that have no counterpart in the original UV Lagrangian but only become apparent in a proper low-energy theory in which the high-energy degrees of freedom are explicitly integrated out. Away from half-filling, a similar state of affairs obtains.

4. Hole Doping: Experimental Consequences

The charge $2e$ boson has much to tell us about the normal state of a doped Mott insulator. Here we compute the electron spectral function, the specific heat, the thermal conductivity, the optical conductivity as well as the dielectric function. In each of these, the charge $2e$ boson produces a distinct signature that accounts for the anomalies of the

doped state of a Mott insulator.

4.1. Spectral Function: Pseudogap

Since we have demonstrated that $\mathcal{L}_{\text{Mott}}$ captures the strong-coupling physics of the Mott insulating state, we focus on the evolution of this theory with doping. The lack of any gradient terms in the action with respect to the bosonic fields and the absence of any bare dynamics associated with φ_i suggests that we can treat φ_i as a homogeneous field. Further, since we are not interested in the dynamics on the Mott scale, we treat φ as a static field. Its sole role is to mix the subsectors which differ in the number of doubly occupied sites. Consequently, our results are valid provided that $\omega < U$ and $U \gg t$. Under these assumptions, the single-particle electron Green function

$$G(k, \omega) = -iFT \langle T c_i(t) c_j^\dagger(0) \rangle, \quad (56)$$

can be calculated rigorously in the path-integral formalism as

$$G(k, \omega) = -iFT \int [D\varphi_i^*][D\varphi_i] \int [Dc_i^*][Dc_i] c_i(t) c_j^*(0) \exp^{-\int \mathcal{L}[c, \varphi] dt}, \quad (57)$$

where FT refers to the Fourier transform and \mathbf{T} is the time-ordering operation. The explicit spin-spin term is not contained in $\mathcal{L}_{\text{Mott}}$. This term will also be dropped in the doped case because even in this limit, the spin-spin term is subdominant (in a naive continuum limit sense) to the other interactions in \mathcal{L} . This state of affairs arises because spin-spin term in $b^\dagger b$ contains four spatial derivatives, whereas the $\varphi^\dagger b$ term contains only two. As a result, all of the physics we present below is associated with the charge rather than the spin degrees of freedom. The continuity of the analysis with that of the half-filled system raises the question that perhaps a fixed point at half-filling persists to finite doping as well in which only the fermion-boson terms are relevant. While our analysis is highly suggestive that such a state of affairs obtains, the possible existence of such a fixed point remains a conjecture as of this writing.

To proceed, we will organize the calculation of $G(k, \omega)$ by first integrating out the fermions (holding φ fixed)

$$G(k, \omega) = \int [D\varphi^*][D\varphi] FT \left(\int [Dc_i^*][Dc_i] c_i(t) c_j^*(0) \exp^{-\int \mathcal{L}[c, \varphi] dt} \right) \quad (58)$$

where now

$$\begin{aligned} \mathcal{L} = & \sum_{i\sigma} (1 - n_{i\bar{\sigma}}) c_{k\sigma}^* \dot{c}_{k\sigma} - \left(2\mu + \frac{s^2}{U} \right) \varphi^* \varphi - \sum_{k\sigma} (g_t t \alpha_k + \mu) c_{k\sigma}^* c_{k\sigma} \\ & + s\varphi^* \sum_k \left(1 - \frac{2t}{U} \right) c_{-k\downarrow} c_{k\uparrow} + c.c. \end{aligned} \quad (59)$$

The effective Lagrangian can be diagonalized and written in terms of a collection of Bogoliubov quasiparticles[11]. The remaining φ integration can then be done numerically to obtain the spectral function.

The spectral functions in Figs. (10) and (11) exhibit four key features. First, there is a low-energy kink in the electron dispersion that is independent of doping. The

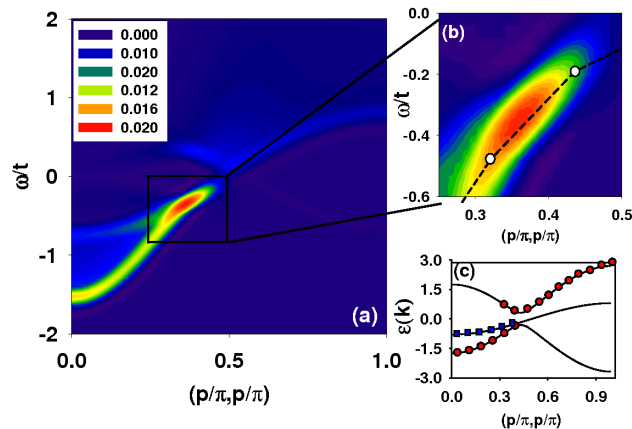


Figure 10. (a) Spectral function for filling $n = 0.9$ along the nodal direction. The intensity is indicated by the color scheme. (b) Location of the low and high energy kinks as indicated by the change in the slope of the electron dispersion. (c) The energy bands that give rise to the bifurcation of the electron dispersion.

low-energy kink occurs at roughly $0.2t \approx 100\text{meV}$. By treating the mass term for the boson as a variable parameter, we verified that the low-energy kink is determined by the bare mass. In the effective low-energy theory, the bare mass is t^2/U . This mass is independent of doping. Experimentally, the low-energy kink[96] does not change with doping. Consequently, the charge $2e$ bosonic field provides a natural mechanism for the kink that is distinct from the phonon schemes that have been proposed[96].

Second, a high-energy kink appears at roughly $0.5t \approx 250\text{meV}$ which closely resembles the experimental kink at 300meV [97]. Cluster[98] and exact diagonalization methods[99] also find a high-energy kink. At sufficiently high doping (see Figs. (11a) and (11b)), the high-energy kink disappears. Third, the electron dispersion bifurcates at the second kink. This is precisely the behaviour that is seen experimentally[97]. The energy difference between the two branches is maximum at $(0, 0)$ as is seen experimentally. A computation of the spectral function at $U = 20t$ and $n = 0.9$ reveals that the dispersion as well the bifurcation still persist. Further, the magnitude of the splitting does not change, indicating that the energy scale for the bifurcation and the maximum energy splitting are set by t and not U . The origin of the two branches is captured in Fig. (10c). The two branches below the chemical potential correspond to the standard band in the LHB (filled squares in Fig. (10c) on which φ vanishes and a branch on which $\varphi \neq 0$ (filled circles in Fig. (10c). Simulations on the Hubbard model clearly resolve either the low-energy feature[92, 93, 94] or the high-energy kink[98, 99]. In the studies showing the high-energy kink, the low-energy feature is not discernible[98, 99]. What is new here is that both features (but with drastically different intensities as is seen experimentally) are captured. The two branches indicate that there are two local maxima in the integrand in Eq. (58), a feature not captured by a saddle-point approximation. Above the chemical potential only one branch survives. The split electron dispersion below the chemical potential is consistent with the composite nature of the electron operator dictated by

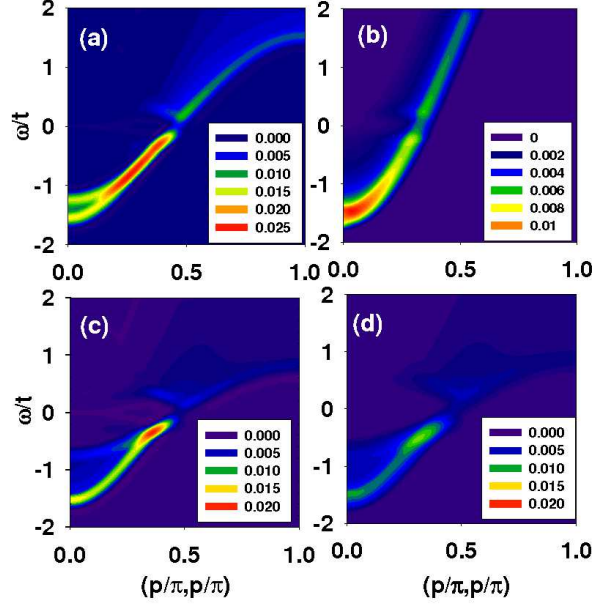


Figure 11. Spectral function for two different fillings (a) $n = 0.8$ and (b) $n = 0.4$ along the nodal direction. The absence of a splitting in the electron dispersion at $n = 0.4$ indicates the bifurcation ceases beyond a critical doping. The spectral functions for two different values of the on-site repulsion, (c) $U = 10t$ and (d) $U = 20t$ for $n = 0.9$ reveals that the high-energy kink and the splitting of the electron dispersion have at best a weak dependence on U . This indicates that this physics is set by the energy scale t rather than U .

Eq. (39). At low energies, the electron is a linear superposition of two states, one the standard band in the LHB described by excitations of the form, $c_{i\sigma}^\dagger(1 - n_{i\bar{\sigma}})$ and the other a composite excitation consisting of a bound hole and the charge $2e$ boson, $c_{i\bar{\sigma}}\varphi_i^\dagger$. The former contributes to the static part of the spectral weight transfer ($2x$) while the new charge e excitation gives rise to the dynamical contribution to the spectral weight transfer. Because the new charge e state is strongly dependent on the hopping, it should disperse as is evident from Fig. (11) and also confirmed experimentally[97].

The formation of the composite excitation, $c_{i\bar{\sigma}}\varphi_i^\dagger$, is the new dynamical degree of freedom in the doped theory. This dynamical degree of freedom has no counterpart in the UV scale. Such a binding of a hole and the charge $2e$ bosonic field leads to a pseudogap at the chemical potential, as evidenced by the absence of spectral weight at the chemical potential for both $n = 0.9$ and $n = 0.8$. Non-zero spectral weight resides at the chemical potential in the heavily overdoped regime, $n = 0.4$, consistent with the vanishing of the pseudogap beyond a critical doping away from half-filling. Because the density of states vanishes at the chemical potential, the electrical resistivity diverges as $T \rightarrow 0$. Such a divergence is shown in Fig. (12a) and is consistent with our previous calculations of the dc resistivity using a local dynamical cluster method[78]. In the absence of the boson (Fig. (12b)), localization ceases. Although this calculation does not constitute a proof, it is consistent with localisation induced by the formation of the

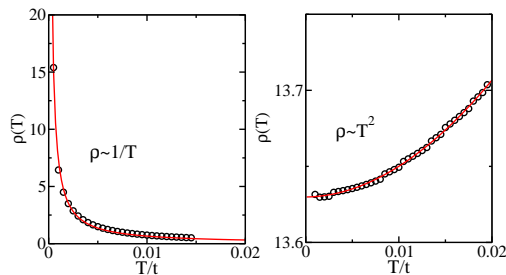


Figure 12. (a)dc electrical resistivity as a function of temperature for $n = 0.9$ (b) Setting the bosonic degree of freedom to zero kills the divergence of the resistivity as $T \rightarrow 0$. This suggests that it is the strong binding between the fermionic and bosonic degrees of freedom that ultimately leads to the insulating behaviour in the normal state of a doped Mott insulator.

bound composite excitation, $c_{i\bar{\sigma}}\varphi_i^\dagger$. This state of affairs obtains because the boson has no bare dynamics. It may acquire dynamics at $O(t^3/U^2)$ as can be seen by expanding the \mathcal{M} matrix in Eq. (38).

Such bound-state formation lays plain how the strong coupling regime of a doped Mott insulator depends on the dimensionality, the doping and the connectivity of the lattice. As the charge $2e$ boson is a local degree of freedom with no bare dynamics, an analogy with bound state formation by a local potential is warranted. It is well known that bound state formation in $d \leq 2$ obtains for an arbitrarily weak local potential. For higher dimensions, a local potential exceeding a threshold value is required for a bound state to form. That such a picture of the bound-state formation applies here is supported by simulations on the Hubbard model. In $d = \infty$ [100] a pseudogap is absent, whereas a variety of strong-coupling cluster methods all yield a pseudogap[101, 102] without invoking symmetry breaking on a $d = 2$ square lattice in the vicinity of half-filling. Since $L > 2x$ is also a signature of a pseudogap (which is mediated by bound-state formation), we conclude that dynamical spectral weight transfer also depends on the dimensionality of the lattice. The absence of a pseudogap in $d = \infty$ implies that there must be some upper critical dimension above which the interactions generated by the t/U corrections in Eq. (16) become irrelevant. The precise nature of this fixed point remains an open problem.

A gap in the spectrum is possible only if the single-particle Green function vanishes along some surface in momentum space. Along such a surface, the self-energy diverges. The imaginary part of the self energy at different temperatures is shown in Fig. (13). At low temperature ($T \leq t^2/U$), the imaginary part of the self-energy at the non-interacting Fermi surface develops a peak at $\omega = 0$. At $T = 0$, the peak leads to a divergence and hence is consistent with the opening of a pseudogap. As we have pointed out earlier[87], a pseudogap is properly identified by a zero surface (the Luttinger surface) of the single-particle Green function. This zero surface is expected to preserve the Luttinger volume if the pseudogap lacks particle-hole symmetry as shown in the second of the figures in Fig. (13).

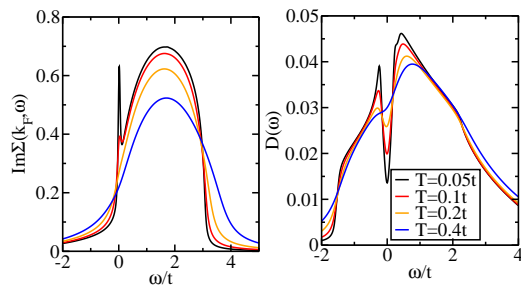


Figure 13. The imaginary part of the self energy as the function of temperature for $n = 0.7$. A peak is developed at $\omega = 0$ at low temperature which is the signature of the opening of the pseudogap. The density of states explicitly showing the pseudogap is shown in adjacent figure.

4.2. Mid-Infrared Band

Naively, doped Mott insulators are expected to either have a far-infrared or an ultra-violet or upper-Hubbard-band scale absorption. Hence, one of the true surprises in the optical response of the cuprates is the mid-infrared band (MIB). While many mechanisms have been proposed[41], no explanation has risen to the fore. A hint as to the origin of this band is that the intensity in the MIB increases with doping at the expense of spectral weight at high energy and the energy scale for the peak in the MIB is the hopping matrix element t . Since the MIB arises from the high-energy scale, the current theory which accurately integrates out the high energy degrees of freedom should capture this physics. We work in the non-crossing approximation,

$$\sigma_{xx}(\omega) = 2\pi e^2 \int d^2k \int d\omega' (2t \sin k_x)^2 \left(-\frac{f(\omega') - f(\omega' + \omega)}{\omega} \right) A(\omega + \omega', k) A(\omega', k),$$

to the Kubo formula for the conductivity where $f(\omega)$ is the Fermi distribution function and $A(\omega, k)$ is the spectral function. In our treatment, the vertex corrections arise solely from the interactions with the bosonic degrees of freedom. Since the boson acquires dynamics only through electron motion and the leading such term is $O(t^3/U^2)$, the treatment here should suffice to provide the leading behaviour of the optical conductivity.

Shown in Fig. (14) is the optical conductivity which peaks at $\omega_{\max} \approx .5t$ forming the MIB. We have subtracted the Drude weight at $\omega = 0$ to focus sharply on the MIB. As the inset indicates, ω_{\max} is an increasing function of the electron filling (n), whereas the integrated weight

$$N_{\text{eff}} = \frac{2m^*}{\pi e^2} \int_0^{\Omega_c} \sigma(\omega) d\omega \quad (60)$$

decreases. However, N_{eff} does not vanish at half-filling indicating that the mechanism that causes the mid-IR is evident even in the Mott state. We set the integration

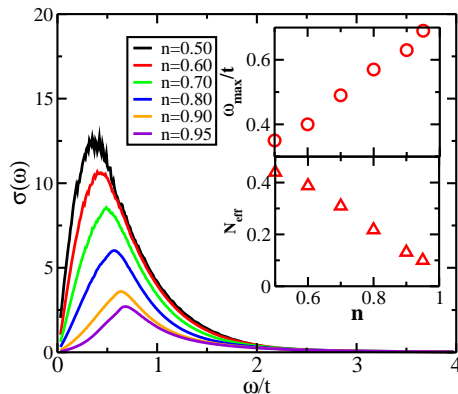


Figure 14. Optical conductivity as a function of electron filling, n with the Drude part subtracted. The peak in the optical conductivity represents the mid-infrared band. Its origin is mobile double occupancy in the lower-Hubbard band. The insets show that the energy at which the MIB acquires its maximum value, ω_{\max} is an increasing function of electron filling. Conversely, the integrated weight of the MIB decreases as the filling increases. This decrease is compensated with an increased weight at high (upper-Hubbard band) energy scale.

cutoff to $\Omega_c = 2t = 1/m^*$. The magnitude and filling dependence of Ω_{\max} are all consistent with that of the mid-infrared band in the optical conductivity in the cuprates[36, 37, 39, 40, 41]. We determined what sets the scale for the MIB by studying its evolution as a function of U . As is clear from Figure (15), ω_{\max} is set essentially by the hopping matrix element t and depends only weakly on J . The physical processes that determine this physics are determined by the coupled boson-Fermi terms in the low-energy theory. The $\varphi_i^\dagger c_{i\uparrow} c_{i\downarrow}$ term has a coupling constant of t whereas the $\varphi_i^\dagger b_i$ scales as t^2/U . Together, both terms give rise to a MIB band that scales as $\omega_{\max}/t = 0.8 - 2.21t/U$ (see inset of Fig. (15)). Since $t/U \approx O(.1)$ for the cuprates, the first term dominates and the MIB is determined predominantly by the hopping matrix element t . Within the interpretation that φ represents a bound state between a doubly occupied site and a hole, second order perturbation theory with the $\varphi_i^\dagger b_i$ term mediates the process shown in Fig. (5). It is the resonance between these two states that results in the mid-IR band. Interestingly, this resonance persists even at half-filling and hence the non-vanishing of N_{eff} at half-filling is not evidence that the cuprates are not doped Mott insulators as has been recently claimed[84].

As the physics in Fig. (5) is not present in projective models which prohibit double occupancy in the Hubbard basis (not simply the transformed fermion basis of the t - J model), it is instructive to see what calculations of the optical conductivity in the $t - J$ model reveal. All existing calculations[40, 82, 77, 83] on the $t - J$ model find that the MIB scales as J . In some of these calculations, superconductivity is needed to induce an MIB[82] also at an energy scale of J . In others, phonons are invoked to overcome the failure of the hard-projected t - J model to yield a mid-infrared band. Experimentally[36, 37, 41], it is clear that the MIB is set by the t scale rather than J . In fact, since the MIB grows at the expense of spectral weight in the upper-Hubbard

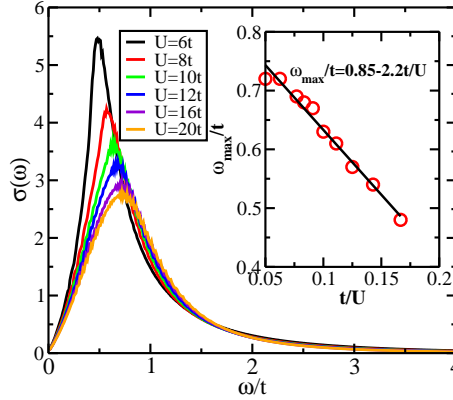


Figure 15. Evolution of the optical conductivity for $n = 0.9$ as U is varied. The inset shows the functional form that best describes ω_{\max} . The dominant energy scale is the hopping matrix element t since t/U for the cuprates is $O(1/10)$.

band, it is not surprising that the t - J model cannot describe this physics as first pointed out by Uchida, et al.[37]. The physical mechanism we have identified here, Fig. (5) clearly derives from the high energy scale, has the correct energy dependence, and hence satisfies the key experimental constraints on the origin of the MIB. Since the physics in Fig. (5) is crucial to the mid-IR, it is not surprising that single-site analysis[84] fail to obtain a non-zero intercept in the extreme Mott limit. The non-zero intercept of N_{eff} is a consequence of Mottness and appears to be seen experimentally in a wide range of cuprates[36, 103, 104, 105].

4.3. Dielectric function: Experimental Prediction

We have shown thus far that there are two branches in the electronic spectral function below the chemical potential. Such physics is explained by the dynamical formation of a new composite excitation, representing a bound state, consisting of a bound hole and a charge $2e$ boson, $\varphi_i^\dagger c_{i\bar{\sigma}}$. We demonstrated that for the MIB in the optical conductivity such an excitation also appears. Such composite charge excitations should show up in response functions which are sensitive to all the charge degrees of freedom, for example, the energy loss function, $\Im 1/\epsilon(\omega, \mathbf{q})$, where $\epsilon(\omega, \mathbf{q})$ is the dielectric function. We show here that this is the case.

To this end, we calculate the inverse dielectric function,

$$\Im \frac{1}{\epsilon(\omega, \mathbf{q})} = \pi \frac{U}{v} \sum_p \int d\omega' (f(\omega') - f(\omega + \omega')) \times A(\omega + \omega', \mathbf{p} + \mathbf{q}) A(\omega', \mathbf{p}),$$

using the non-crossing approximation discussed earlier. Our results are shown in Fig.(16) for $n = 0.9$ and $n = 0.6$ for \mathbf{q} along the diagonal. Two features are distinct. First, there is a broad band (red arrow in Fig. (16)) with the width of order t that disperses with \mathbf{q} for both doping levels. It is simply the particle-hole continuum which arises from the renormalized bare electron band. The band width is doping dependent as a

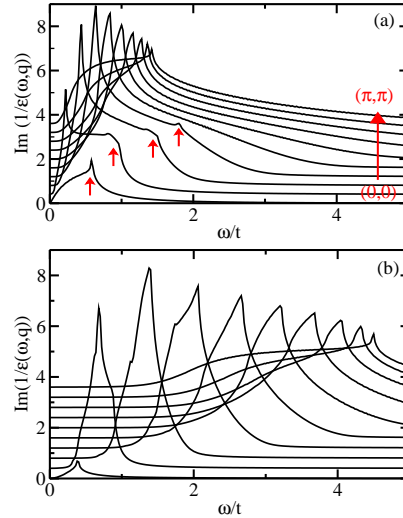


Figure 16. The dielectric function, $-\Im 1/\epsilon(\omega, \mathbf{q})$ for \mathbf{q} along the diagonal direction is shown for (a) $n = 0.9$ and (b) $n = 0.6$. Note only the broad feature indicated by the red arrow at $n = 0.9$ persists at $n = 0.6$.

result of the renormalization of the band with doping. More strikingly, for $n = 0.9$, a sharp peak exists at $\omega/t \approx .2t$. It disperses with q , terminating when $\mathbf{q} \rightarrow (\pi, \pi)$. Physically, the sharp peak represents a quasiparticle excitation of the composite object, $\varphi_i^\dagger c_{i\bar{\sigma}}$, the charge $2e$ boson and a hole. Therefore, we predict that if this new composite charge excitation, $\varphi_i^\dagger c_{i\bar{\sigma}}$, is a real physical entity, as it seems to be, it will give rise to a sharp peak in addition to the particle-hole continuum in the inverse dielectric function. Since this function has not been measured at present, our work here represents a prediction. Electron-energy loss spectroscopy can be used to measure the inverse dielectric function. Our key prediction is that momentum-dependent scattering should reveal a sharp peak that appears at low energy in a doped Mott insulator. We have checked numerically the weight under the peaks in the inverse dielectric function and the sharp peak is important. Hence, the new charge e particle we have identified here should be experimentally observable. The two dispersing particle-hole features found here are distinct from a similar feature in stripe models[106]. In such models the second branch[106] has vanishing weight and whereas in the current theory both features are of unit weight.

4.4. Heat conductivity and heat capacity

Loram and collaborators[107] have shown from their extensive measurements that the heat capacity in the cuprates in the normal state scales as T^2 . It is a trivial exercise to show that such a temperature dependence requires a V-shaped gap density of states as a function of energy. The slope of the density of states in the vicinity of the chemical potential determines the coefficient of the T^2 term. Because the slope of the density of

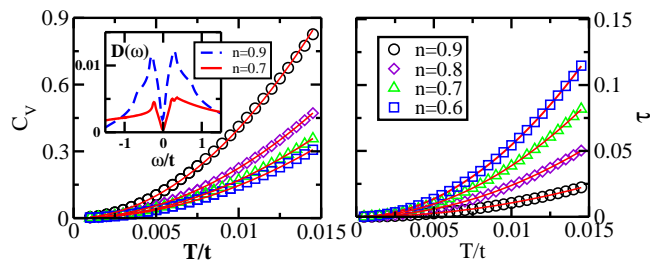


Figure 17. (a) Heat capacity, C_V , and (b) thermal conductivity, τ , calculated at $n = 0.9$. The solid lines are a fit to T^2 . Inset: Density of states for $U = 10t$ are evaluated at $n = 0.9$ and $n = 0.7$ respectively.

states decreases as the pseudogap closes, the magnitude of the T^2 term should diminish as the doping increases. As we showed in the previous section, the boson creates a pseudogap. The energy dependence of the gap is shown in the inset of Fig. (17). A linear dependence on energy is apparent. We calculated the heat capacity shown in Fig.(17a) via the relationship $C_v = \frac{d\bar{E}}{dt}$, where the internal energy, \bar{E} , is

$$\bar{E} = \int d\omega D(\omega)\omega f(\omega) \quad (61)$$

and $D(\omega) = \sum_{\mathbf{k}} A(\omega, \mathbf{k})$. As expected, the temperature dependence is quadratic in the doping regime where the pseudogap is present as is seen experimentally[107]. As it is the boson that underlies the pseudogap, it is the efficient cause of the T^2 dependence of the heat capacity. In our theory, the steeper slope occurs at smaller doping which gives rise to the largest heat capacity at half filling. This doping dependence of the heat capacity seems to contradict the experimental observations[107]. A key in determining the magnitude of the heat capacity is the spin degrees of freedom. As we have focused entirely on the bosonic degree of freedom and not on the contribution from the spin-spin interaction terms, we have over-estimated the kinetic energy. Such terms do not affect the pseudogap found here though they do change the doping dependence[77]. From Eq. (39) it is clear that the spin-spin terms renormalize the standard fermionic branch in the lower-Hubbard band leaving the new state mediated by φ_i untouched.

Additionally, the thermal conductivity, $\tau(T)$, can be calculated using the Kubo formula in non-crossing approximation,

$$\tau(T) = \frac{e}{4k_B T} \sum_{\mathbf{k}} \int \frac{d\omega}{2\pi} (v_{\mathbf{k}}^x)^2 \omega^2 \left(-\frac{\partial f(\omega)}{\partial \omega} \right) A(\mathbf{k}, \omega)^2.$$

The thermal conductivity shown in Fig.(17) scales as T^2 which is identical to that of the heat capacity. However, the system exhibits a larger thermal conductivity as the doping increases in contrast to the heat capacity which is decreasing as the doping increases. Physically, this signifies that the carriers are more mobile as the doping increases.

4.5. T -linear Resistivity

A key theme of this review is that the normal state of doped Mott insulators is dominated by dynamical degrees of freedom that could not have been deduced from the UV physics. Further, as stated in the introduction, the correct theory of the pseudogap phase should also explain the T -linear resistivity. The standard explanation[108] attributes T -linear resistivity to quantum criticality. However, one of us has recently shown[108] that under three general assumptions, 1) one-parameter scaling, 2) the critical degrees of freedom carry the current and 3) charge is conserved, the resistivity in the quantum critical regime takes the universal form,

$$\sigma(\omega = 0) = \frac{Q^2}{\hbar} \Sigma(0) \left(\frac{k_B T}{\hbar c} \right)^{(d-2)/z}. \quad (62)$$

As a result, quantum criticality in its present form yields T -linear resistivity (for $d=3$) only if the dynamical exponent satisfies the unphysical constraint $z < 0$. The remedy here might be three-fold: 1) some other yet-unknown phenomenon is responsible for T -linear resistivity, 2) the charge carriers are non-critical, or 3) the single-parameter scaling hypothesis must be relaxed.

The new dynamical degree of freedom we have identified here fits the bill and provides the added ingredient to explain T -linear resistivity. While none of the calculations presented here is sufficient to account for the confined dynamics of φ_i , the formation of the pseudogap, the divergence of the electrical resistivity, the $\varphi_i^\dagger c_{i\bar{\sigma}}$ feature in the electron operator, and the new feature in the dielectric function all point in this direction. Consequently, we assume that $\varphi_i^\dagger c_{i\bar{\sigma}}$ forms a bound state and the binding energy is E_B . As a bound state, $E_B < 0$, where energies are measured relative to the chemical potential. Upon increased hole doping, the chemical potential decreases. Beyond a critical doping, the chemical potential, crosses the energy of the bound state. At the critical value of the doping where $E_B = 0$, the energy to excite a boson vanishes. The critical region is dominated by electron-boson scattering. In metals, it is well-known[109] that above the Debye temperature, the resistivity arising from electron-phonon scattering is linear in temperature. We make a direct analogy here with the electrons scattering off phonons in a metal. Once the boson unbinds, we assume its dynamics is purely classical. Since the energy to create a boson vanishes at criticality as shown in Fig. (18), T -linear resistivity obtains. Namely, in the critical region, the energy to create a boson vanishes as shown in Fig. (18) and hence the resistivity arising from electron-boson scattering should be linear in temperature. This mechanism is robust (assuming the unbound boson has classical dynamics) as it relies solely on the vanishing of the boson energy at criticality and not on the form of the coupling. To the right of the quantum critical point, standard electron-electron interactions dominate and Fermi liquid behaviour obtains. In this scenario, the quantum critical point coincides with the termination of the pseudogap phase, or equivalently with the unbinding of the bosonic degrees of freedom. Since it is the bound state of the boson that creates the new charge e state giving rise to $L/n_h > 1$ and this state is generated as a result of dynamical

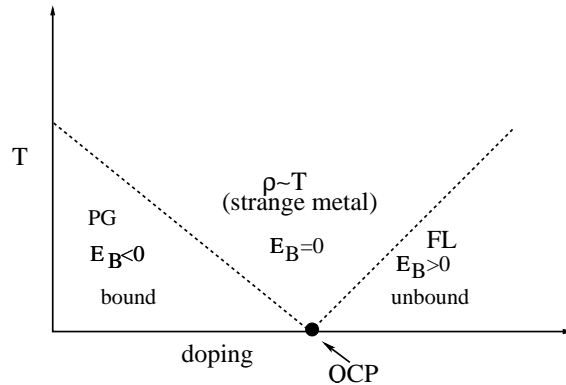


Figure 18. Proposed phase diagram for the binding of the holes and bosons that result in the formation of the pseudogap phase. Once the binding energy vanishes, the energy to excite a boson vanishes. In the critical regime, the dominant scattering mechanism is still due to the interaction with the boson. T-linear resistivity results anytime $T > \omega_b$, where ω_b is the energy to excite a boson. To the right of the quantum critical regime (QCP), the boson is irrelevant and scattering is dominated by electron-electron interactions indicative of a Fermi liquid. The QCP signifies the end of the binding of fermi and bosonic degrees of freedom that result in the pseudogap phase.

spectral weight transfer, the T^* line defines the temperature below which dynamical spectral weight transfer contributes to the low-energy spectral weight. Consequently, the mechanism proposed here is experimentally testable. Simply repeat the x-ray K-edge experiments presented in Fig. (3) below and above the T^* line. Above T^* the integrated weight should be $2x$ whereas below it should exceed $2x$.

4.6. Towards Superconductivity

Our emphasis thus far has been on identifying a unifying principle for the normal state of the cuprates. As we have seen, strong correlations mediate new composite excitations made partly out of the emergent charge $2e$ boson that results by exactly integrating out the high-energy scale in the Hubbard model. An important question concerns the relevance of the physics we have identified here to the superconducting phase. Equivalently, what role, if any, does dynamical spectral weight transfer play in the superconducting state? We answer this question by focusing on a correlate of high-temperature superconductivity. As the phase diagram indicates, the superconducting region is roughly dome-shaped. Why superconductivity peaks at a particular doping level is not known. To offer some insight into this puzzle, we focus on an experimental quantity which exhibits an abrupt sign change near optimal doping. As shown in Fig. (19), at a doping level corresponding to the highest superconducting transition temperature for a wide range of cuprates, the thermopower vanishes[110]. Consequently, the sign change of S occurs at the doping value defining the top of the “dome”. While this might be an accident, the fact that the thermopower vanishes at the same doping level for most cuprates indicates that the reason might have something to do with the superconducting mechanism.

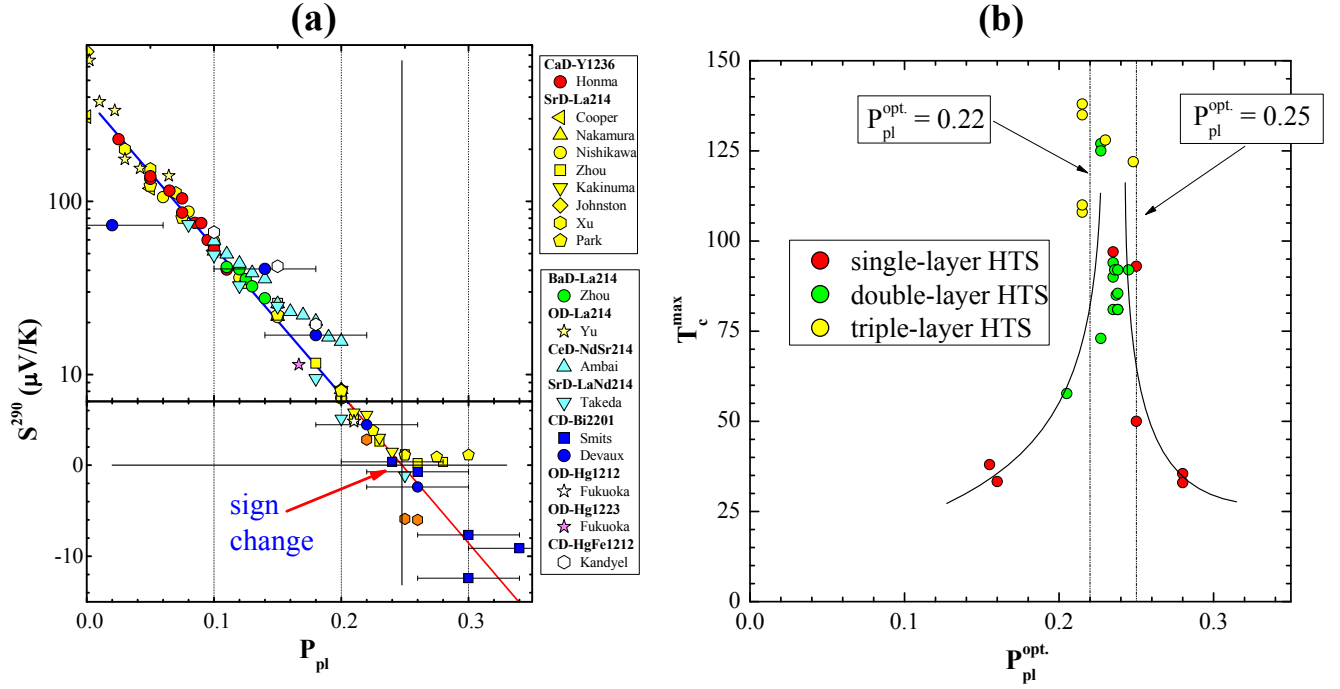


Figure 19. a) Universal behavior of the thermoelectric power[110] (290K) as a function of planar hole density (P_{pl}), for various families of hole-doped cuprates. All exhibit a sign change at $P_{pl} = 0.23$. Above the solid-bold horizontal line, the thermopower obeys the functional form, $S^{290}(P_{pl}) = 392 \exp(-19.7P_{pl})$ for $0.01 < P_{pl} < 0.21$. Below the solid-bold horizontal line, $S^{290}(P_{pl}) = 40.47 - 163.4P_{pl}$ for $0.21 < P_{pl} < 0.34$. These functional forms were used[110] to determine the hole doping levels for all the cuprates rather than the widely used empirical formula[111] $1 - T_c/T_c^{\text{max}} = 82.6(x - 0.16)^2$ which artificially fixes the optimal doping level of all cuprates to be 0.16. The thermopower scale is unbiased in this regard and has been shown[110] to corroborate independent measures of the doping level even in Y123 and Tl-2201 in which it is the oxygen content that determines the doping level. b) Maximum transition temperature as a function of the planar hole density using the thermopower scale to determine the doping level. Except for three single-layer materials, the vanishing of the thermopower coincides with the doping level at which the transition temperature is maximized.

The thermopower measures the thermoelectric voltage induced across a material in response to an applied temperature gradient. Microscopically, the thermopower is a measure of the entropy per charge carrier. Further, it reveals the nature of the dominant charge carriers, being positive for holes and negative for electrons. Should the entropy per carrier be identical for particles and holes, the thermopower vanishes. Consider hole-doping a Mott insulator. Because transport obtains in the lower-Hubbard band, naively a vanishing of the thermopower is expected whenever the number of states above and below the chemical potential is equal. In the atomic limit, this corresponds to the condition $2x = 1 - x$, the solution of which is $x_{\text{crit}} = 1/3$. This result is corroborated by the large U limit of the thermopower,

$$S = -\frac{k_B}{e} \ln \frac{2x}{1-x}, \quad (63)$$

computed by Beni[112] roughly 20 years before spectral weight transfer was discovered. Since $2x$ and $1 - x$ are the exact values for the electron addition and removal states, respectively, in the atomic limit, it is easy to see that the logarithm is precisely the entropy per carrier. The logarithm vanishes at $x_{\text{crit}} = 1/3$ which is the exact particle-hole symmetric condition for the LHB in the atomic limit. Finite t/U corrections will increase L and as a result decrease x_{crit} . However, this is not all. The spectral function is strongly momentum dependent when $t/U \neq 0$. As a result, strict particle-hole symmetry is not needed to make the thermopower (or even the Hall coefficient) vanish as can be seen directly from the exact[113] expression. Both of these effects conspire[113] to move the doping level at which the thermopower vanishes significantly below the atomic limit of $x = 1/3$. As this change is made entirely from the t/U corrections to the thermopower, it is the dynamical spectral weight transfer that is ultimately responsible for the precise value of doping at which the thermopower vanishes in the cuprates. Consequently, the dynamical spectral weight transfer plays a role in maximizing T_c . As a result, superconductivity in the cuprates is determined fundamentally by the mixing between the high and low energy scales in a doped Mott insulator. The collective degree of freedom φ which results from the spectral weight transfer is consequently central to the superconducting mechanism. Optical conductivity experiments[114, 115, 116] certainly have shown this plainly that the onset of superconductivity results in a decrease in the spectral weight in the UHB. It would seem then that the ultimate solution to superconductivity hinges on the precise dynamics of the collective charge $2e$ boson that we have shown to exist in the exact low-energy theory of a doped Mott insulator.

Acknowledgments

This research was supported in part by the NSF DMR-0605769, P. H. Hor and T. Honma for the use of their thermopower data and S. Chakraborty his characteristically level-headed remarks. P. Phillips thanks the Max-Planck Institute in Dresden for their hospitality during the writing of this article.

- [1] Mott N F, 1949 The Basis of the electron theory of metals, with special reference to transition metals Proc. Phys. Soc. London, Series A **62**, 416-422.
- [2] Hybertsen M S, Stechel E B, Schluter M, and Jennison D R 1990 Renormalization from density-functional theory to strong-coupling models for electronic states in Cu-O material Phys. Rev. B **41** 11068 - 11072.
- [3] Hubbard J. 1964 Electron correlations in narrow bands. III. An Improved Solution Proc. Roy. Soc. London, Ser. A **281** 401-419.
- [4] Harris A B and Lange R V 1967 Single-Particle Excitations in Narrow Energy Bands Phys. Rev. **157** 295-314.
- [5] Kaplan T A, Horsch P, and Fulde P 1982 Close Relation between localized-electron magnetism and the paramagnetic wave function of completely itinerant electrons Phys. Rev. Lett. **49** 889-892.
- [6] Castellani C, Di Castro C, Feinberg D, and Ranninger J 1979 New Model Hamiltonian for the Metal-Insulator Transition Phys. Rev. Lett. **43** 1957 - 1960.
- [7] Alloul H, Ohno T, and Mendels P 1989 89Y NMR evidence for a fermi-liquid behavior in $\text{YBa}_2\text{Cu}_3\text{O}_{6+x}$ Phys. Rev. Lett. **63** 1700-1703.
- [8] Norman M R, Ding H, Randeria M, Campuzano J C, Yokoya T, Takeuchi T, Takahashi T,

- Mochiku T, Kadowaki K, Guptasarma P and Hinks D G 1998 Destruction of the Fermi surface in underdoped high- T_c superconductors *Nature (London)* **392** 157-160.
- [9] Leigh R G, Phillips P, and Choy T P 2007 Hidden charge 2e boson in doped Mott insulators *Phys. Rev. Lett.* **99** 046404/1-4.
- [10] Choy T P, Leigh R G, Phillips P, and Powell P D. 2008 Exact integration of the high-energy scale in a doped Mott insulator *Phys. Rev. B* **77**, 014512/1-12.
- [11] Choy T P, Leigh R G, Phillips P, 2008 Charge 2e boson: Experimental consequences for doped Mott insulators, *Phys. Rev. B* **77**, 104524/1-9.
- [12] Kanigel A, Norman M R, Randeria M, Chatterjee U, Souma S, Kaminski A, Fretwell H M, Rosenkranz S, Shi M, Sato T, Takahashi T, Li Z Z, Raffy H, Kadowaki K, Hinks D, Ozyuzer L, Campuzano J C 2006 Evolution of the pseudogap from Fermi arcs to the nodal liquid *Nat. Phys.* **2** 447-451.
- [13] Timusk T and Statt B 1999 The pseudogap in high-temperature superconductors: an experimental survey *Rep. Prog. Phys.* **62** 61-122.
- [14] For a review, see Batlogg B, Takagi H, Kao H L, and Kwo J, *Electronic Properties of High- T_c Superconductors*, edited by Kuzmany H, Mehring M and Fink J, Springer-Verlag, Berlin, 1993 pp. 5-12.
- [15] Ando Y, Komiya S, Segawa K, Ono S, and Kurita Y 2004 Electronic Phase Diagram of High- T_c Cuprate Superconductors from a Mapping of the In-Plane Resistivity Curvature *Phys. Rev. Lett.* **93** 267001/1-4.
- [16] Kivelson S A, Fradkin E, Emery V J 1998 Electronic liquid-crystal phases of a doped Mott insulator *Nature* **393** 550-553.
- [17] Chakravarty S, Laughlin R B, Morr Dirk K and Chetan Nayak 2001 Hidden order in the cuprates *Phys. Rev. B* **63** 094503/1-10.
- [18] Anderson P W 1987 The Resonating Valence Bond State in La_2CuO_4 and Superconductivity *Science* **235** 1196 - 1198.
- [19] Emery V J and Kivelson S A 1995 Importance of phase fluctuations in superconductors with small superfluid density *Nature* **374** 434-437.
- [20] Randeria M, Trivedi N, Moreo A and Scalettar R T 1992 Pairing and spin gap in the normal state of short coherence length superconductors *Phys. Rev. Lett.* **69** 2001-2004.
- [21] Ranninger J, Robin J M and Eschrig M 1995 Superfluid Precursor Effects in a Model of Hybridized Bosons and Fermions *Phys. Rev. Lett.* **74** 4027-4030.
- [22] Franz M and Tesanovic Z 2001 Algebraic Fermi liquid from phase fluctuations: Topological fermions, vortex berryons and QED3 Theory of Cuprate Superconductors *Phys. Rev. Lett.* **87** 257003/1-4.
- [23] Xu Z A, Ong N P, Wang Y, Kakeshita T and Uchida S 2000 Vortex-like excitations and the onset of superconducting phase fluctuation in underdoped $\text{La}_{2-x}\text{Sr}_x\text{CuO}_4$ *Nature* **406** 486-488.
- [24] Kanigel A, Chatterjee U, Randeria M, Norman M R, Koren G, Kadowaki K, and Campuzano J C 2008 Evidence for pairing above T_c from the dispersion in the pseudogap phase of cuprates [arXiv:0803.3052](https://arxiv.org/abs/0803.3052).
- [25] Tranquada J M, Woo H, Perring T G, Goka H, Gu G D, Xu G, Fujita M and Yamada K 2004 Quantum magnetic excitations from stripes in copper oxide superconductors *Nature* **429**, 534-538.
- [26] Zaanen J and Gunnarsson O 1989 Charged magnetic domain lines and the magnetism of high- T_c oxides *Phys. Rev. B* **40** 7391-7394.
- [27] Abbamonte P, Rusydi A, Smadici S, Gu G D, Sawatzky G A, and Feng D L 2005 Spatially modulated 'Mottness' in $\text{La}_{2-x}\text{Ba}_x\text{CuO}_4$ *Nat. Phys.* **1** 155-158.
- [28] Fink J, Schierle E, Weschke E, Geck J, Hawthorn D, Wadati H, Hu H H, Durr H A, Wizent N, Buchner B, and Sawatzky G A 2008 Charge order in $\text{La}_{1.8-x}\text{Eu}_{0.2}\text{Sr}_x\text{CuO}_4$ studied by resonant soft X-ray diffraction [arXiv:0805.4352](https://arxiv.org/abs/0805.4352).
- [29] Pasupathy A N, Pushp A, Gomes K K, Parker C V, Wen J, Xu Z, Gu G, Ono S, Ando Y, and

- Yazdani A 2008 Electronic Origin of the Inhomogeneous Pairing Interaction in the High-Tc Superconductor $\text{Bi}_2\text{Sr}_2\text{CaCu}_2\text{O}_{8+\delta}$ *Science* **320** 196-201.
- [30] Jing X, Elizabeth S, Deutscher G, Kivelson S A, Bonn D A, Hardy W N, Liang R, Siemons W, Koster G, Fejer M M, Kapitulnik A. 2008 Polar Kerr-Effect Measurements of the High-Temperature $\text{YBa}_2\text{Cu}_3\text{O}_{6+x}$ Superconductor: Evidence for Broken Symmetry near the Pseudogap Temperature 2008 *Phys. Rev. Lett* **100** 127002.
- [31] Kaminski A, Fretwell H M, Campuzano J C, Li Z, Raffy H, Cullen W G, You H, Olson C G, Varma C M and Höchelt H 2002 Spontaneous breaking of time-reversal symmetry in the pseudogap state of a high-Tc superconductor *Nature* **416** 610-613.
- [32] Simon M E and Varma C M 2002 Detection and Implications of a Time-Reversal Breaking State in Underdoped Cuprates *Phys. Rev. Lett.* **89** 247003/1-4.
- [33] Fauque B, Sidis Y, Hinkov V, Pailhe S, Lin C T, Chaud X, and Bourges P 2006 Resonant Magnetic Excitations at High Energy in Superconducting $\text{YBa}_2\text{Cu}_3\text{O}_{6.85}$ *Phys. Rev. Lett.* **96** 197001/1-4.
- [34] Leyraud N D, Proust C, LeBoeuf D, Levallois J, Bonnemaïson J B, Liang R, Bonn D A, Hardy W N, and Taillefer L 2007 Quantum oscillations and the Fermi surface in an underdoped high-Tc superconductor *Nature* **447** 565-568.
- [35] Konstantinovic Z, Li Z Z, and Raffy H 2001 Evolution of the resistivity of single-layer $\text{Bi}_2\text{Sr}_{1.6}\text{La}_{0.4}\text{CuO}_y$ thin films with doping and phase diagram *Physica C* **351** 163-168.
- [36] Cooper S L, Thomas G A, Orenstein J, Rapkine D H, Millis A J, Cheong S W, Cooper A S and Fisk Z 1990 Growth of the optical conductivity in the Cu-O planes *Phys. Rev. B* **41** 11605-11608; Cooper S L, Reznik D, Kotz A, Karlow M A, Liu R, Klein M V, Lee W C, Giapintzakis J, Ginsberg D M, Veal B W and Paulikas S P 1993 Optical studies of the a-, b-, and c-axis charge dynamics in $\text{YBa}_2\text{Cu}_3\text{O}_{6+x}$ *Phys. Rev. B* **47** 8233-8248.
- [37] Uchida S, Ido T and Takagi H, Arima T, Tokura Y and Tajima S 1991 Optical spectra of $\text{La}_{2-x}\text{Sr}_x\text{CuO}_4$: Effect of carrier doping on the electronic structure of the CuO₂ plane *Phys. Rev. B* **43** 7942-7954.
- [38] van der Marel D, Molegraaf H J A, Zaanen J, Nussinov Z, Carbone F, Damascelli A, Eisaki H, Greven M, Kes P H and Li M 2003 Quantum critical behaviour in a high-Tc superconductor *Nature* **425** 271-274.
- [39] Moore S W, Graybeal J M, Tanner D B, Sarrao J, and Fisk Z 2002 Optical properties of $\text{La}_2\text{Cu}_{1-x}\text{Li}_x\text{O}_4$ in the mid-infrared *Phys. Rev. B* **66** 060509/1-4.
- [40] Bouvier J, Bontemps N, Gabay M, Nanot M and Queyroux F 1992 Infrared reflectivity versus doping in $\text{YBa}_2\text{Cu}_3\text{O}_{6+x}$ and $\text{Nd}_{1+y}\text{Ba}_{2-y}\text{Cu}_3\text{O}_{6+x}$ ceramics: Relationship with the t-J model *Phys. Rev. B* **45** 8065-8073.
- [41] Lee Y S, Segawa K, Li Z Q, Padilla W J, Dumm M, Dordevic S V, Homes C C, Ando Y, and Basov D N 2005 Electrodynamics of the nodal metal state in weakly doped high-Tc cuprates , *Phys. Rev. B* **72** 054529/1-13.
- [42] Polchinski J 1992 Effective Field Theory and the Fermi Surface hep-th/9210046.
- [43] Benfatto G and Gallavotti G 1990 Perturbation theory of the Fermi surface in a quantum liquid: A general quasiparticle formalism and one-dimensional systems *J. Stat. Phys.* **59** 541-664.
- [44] Benfatto G and Gallavotti G 1990 Renormalization-group approach to the theory of the Fermi surface *Phys. Rev. B* **42** 9967-9972.
- [45] Shankar R 1991 Renormalization group for interacting fermions in $d > 1$ *Physica* **A177** 530-536; Volovik G E 2007 “Quantum Analogues: From Phase Transitions to Black Holes and Cosmology”, eds. Unruh W G and Schutzhold R, Springer Lecture Notes in Physics 718/2007, pp. 31-73.
- [46] Möller G, Ruckenstein A E and Schmitt-Rink S 1992 Transfer of spectral weight in an exactly solvable model of strongly correlated electrons in infinite dimensions *Phys. Rev. B* **46** 7427-7432.
- [47] Laughlin R B 1998 A Critique of Two Metals *Adv. Phys.* **47** 943-958.
- [48] Slater J C 1951 Magnetic Effects and the Hartree-Fock Equation *Phys. Rev.* **82** 538-541.

- [49] Kuiper P, Kruizinga G, Ghijsen J, and Sawatzky G A 1989 Character of Holes in $\text{Li}_x\text{Ni}1 - x\text{O}$ and Their Magnetic Behavior *Phys. Rev. Lett.* **62** 221-224.
- [50] Eskes H, Tjeng L H and Sawatzky G A 1990 Cluster-model calculation of the electronic structure of CuO : A model material for the high- T_c superconductors *Phys. Rev. B* **41** 288-299.
- [51] Varma C M, Schmitt-Rink S, Abrahams E 1987 Charge transfer excitations and superconductivity in ionic metals *Solid State Comm.* **62** 681-685.
- [52] Emery V J 1987 Theory of high- T_c superconductivity in oxides *Phys. Rev. Lett.* **58** 2794-2797.
- [53] Chen C T, Sette F, Ma Y, Hybertsen M S, Stechel E B, Foulkes W M C, Schuller M, Cheong S W, Cooper A S, Rupp L W, Batlogg B, Soo Y L, Ming Z H, Krol A and Kao Y H 1991 Electronic states in $\text{La}_{2-x}\text{Sr}_x\text{CuO}_{4+\delta}$ probed by soft-x-ray absorption *Phys. Rev. Lett.* **66** 104-107.
- [54] Meinders M B J, Eskes H, and Sawatzky G A 1993 Spectral-weight transfer: Breakdown of low-energy-scale sum rules in correlated systems *Phys. Rev. B* **48**, 3916-3926.
- [55] Hybertsen M S, Stechel E B, Foulkes W M C and Schlüter M 1992 Model for low-energy electronic states probed by x-ray absorption in high- T_c cuprates *Phys. Rev. B* **45**, 10032-10050.
- [56] Kapit E and LeClair A 2008 A unique non-Landau/Fermi liquid in 2d for high T_c superconductivity [arXiv:0805.2951](https://arxiv.org/abs/0805.2951).
- [57] Tye S H 2008 On the New Model of Non-Fermi Liquid for High Temperature Superconductivity [arXiv:0805.4200](https://arxiv.org/abs/0805.4200).
- [58] Stanescu T D, Galitski, and Drew H D, 2008 Effective masses in a strongly anisotropic Fermi liquid *Phys. Rev. Lett.* **101** 066405 (2008).
- [59] Stanescu T D and Kotliar G, 2006 Fermi arcs and hidden zeros of the Green function in the pseudogap state *Phys. Rev. B* **74** 125110/1-4.
- [60] Lee P A, Nagaosa N, Wen, X -G, 2006 Doping a Mott insulator: Physics of high-temperature superconductors *Rev. Mod. Phys.* **78** 17-86.
- [61] Anderson P W 2006 The 'strange metal' is a projected Fermi liquid with edge singularities *Nat. Phys.* **3** 626-630.
- [62] Kotliar G. and Ruckenstein A E 1986 New functional integral approach to strongly correlated Fermi systems: The Gutzwiller approximation as a saddle point *Phys. Rev. Lett.* **57** 1362-1365.
- [63] Eskes H, Oleś A M, Meinders M B J, Stephan W, 1994 Spectral properties of the Hubbard bands *Phys. Rev. B* **50**, 17980-18002.
- [64] Phillips P, Galanakis D, and Stanescu T D 2004 Absence of Asymptotic Freedom in Doped Mott Insulators: Breakdown of Strong Coupling Expansions *Phys. Rev. Lett.* **93** 267004.
- [65] Chao K A, Spalek J, and Oleś A M 1977 Kinetic exchange interaction in a narrow S-band *J. Phys. C.* **10** L271-L588.
- [66] MacDonald A H, Girvin S M, and Yoshioka D 1988 t/U expansion for the Hubbard model *Phys. Rev. B* **37**, 9753-9756.
- [67] Chernyshev A L, Galanakis D, Phillips P, Rozhkov A V and Tremblay A M S 2004 Higher order corrections to effective low-energy theories for strongly correlated electron systems *Phys. Rev. B* **70** 235111/1-12.
- [68] Anderson P W 1959 New Approach to the Theory of Superexchange Interactions *Phys. Rev.* **115** 2-13.
- [69] Zhang F C and Rice T M, 1989 Effective Hamiltonian for the superconducting Cu oxides *Phys. Rev. B* **37**, 3759-3762.
- [70] Dagotto E, Fradkin E, and Moreo A 1988 $\text{SU}(2)$ gauge invariance and order parameters in strongly coupled electronic systems *Phys. Rev. B* **38** 2926-2929.
- [71] Affleck I, Zou Z, Hsu T, and Anderson P W 1988 $\text{SU}(2)$ gauge symmetry of the large- U limit of the Hubbard model *Phys. Rev. B* **38** 745-747.
- [72] Kane C L, Lee P A and Read N 1989 Motion of a single hole in a quantum antiferromagnet *Phys. Rev. B* **39** 6880-6897.
- [73] Dagotto E 1994 Correlated electrons in high-temperature superconductors *Rev. Mod. Phys.* **66** 763-840.

- [74] Mishchenko, A S, Prokof'ev N V and Svistunov B V (2001) Single-hole spectral function and spin-charge separation in the t-J model Phys. Rev. B **64**, 033101/1-4.
- [75] Sorella S 1992 Quantum Monte Carlo study of a single hole in a quantum antiferromagnet Phys. Rev. B **46** 11670-11680.
- [76] Haule K, Rosch A, Kroha J, and Wolfle P 2003 Pseudogaps in the t-J model: An extended dynamical mean-field theory study Phys. Rev. B **68** 155119/1-19.
- [77] Zemljic M M and Prelovsek P 2005 Resistivity and optical conductivity of cuprates within the t-J model Phys. Rev. B **72** (2005) 075108/1-8.
- [78] Choy T P and Phillips P 2005 Doped Mott Insulators Are Insulators: Hole Localization in the Cuprates Phys. Rev. Lett. **95** 196405/1-4.
- [79] Kawakami N and Yang S K 1990 Correlation functions in the one-dimensional t-J model Phys. Rev. Lett. **65**, 2309-2312.
- [80] Kawakami N and Yang S K 1990 Luttinger anomaly exponent of momentum distribution in the Hubbard chain Phys. Lett. A **148**, 359-362.
- [81] Frahm H and Korepin V E 1990 Critical exponents for the one-dimensional Hubbard model Phys. Rev. B **42**, 10553-10565.
- [82] Haule K and Kotliar G 2007 Optical conductivity and kinetic energy of the superconducting state: A cluster dynamical mean field study Europhys. Lett. **77** 27007-27010.
- [83] Mischenko A S, Nagaosa N, Shen Z X, De Filippis G, Cauaudella V, Devereaux T P, Bernhard C, Kim K W, and Zaanen J 2008 Charge Dynamics of Doped Holes in High Tc Cuprate Superconductors: A Clue from Optical Conductivity Phys. Rev. Lett. **100** 166401/1-4.
- [84] Comanac A, de Medici L, Capone M, and Millis A J 2008 Optical conductivity and the correlation strength of high-temperature copper-oxide superconductors Nat. Phys. **4** 287-290.
- [85] Chakraborty S, Galanakis D, and Phillips P 2008 Kinks and Mid-Infrared Optical Conductivity from Strong Electron Correlation arXiv:0712.2838.
- [86] Dzyaloshinskii I 2003 Some consequences of the Luttinger theorem: The Luttinger surfaces in non-Fermi liquids and Mott insulators Phys. Rev. B **68**, 85113/1-6.
- [87] Phillips P 2006 Mottness Ann. of Phys. **321** 1634-1650.
- [88] Stanescu T D, Phillips P, and Choy T P 2007 Theory of the Luttinger surface in doped Mott insulators Phys. Rev. B **75** 104503/1-9.
- [89] Essler F H L and Tselik A, 2003 Finite Temperature Spectral Function of Mott Insulators and Charge Density Wave States Phys. Rev. Lett. **90**126401/1-4
- [90] Bohm D and Pines D 1953 A Collective Description of Electron Interactions: III. Coulomb Interactions in a Degenerate Electron Gas Phys. Rev. **92** 609-625.
- [91] Murthy G and Shankar R, 2003 Hamiltonian theories of the fractional quantum Hall effect Rev. Mod. Phys. **75**, 1101-1158.
- [92] Moukouri S and Jarrell M, 2001 Absence of a Slater Transition in the Two-Dimensional Hubbard Model Phys. Rev. Lett. **87** 167010/1-4.
- [93] Civelli M, Capone M, Kancharla S S, Parcolet O, and Kotliar G 2005 Dynamical Breakup of the Fermi Surface in a Doped Mott Insulator Phys. Rev. Lett. **95** 106402/1-4.
- [94] Maier T, Jarrell M, Pruschke T, and Hettler M H 2005 Rev. Mod. Phys. **77** 1027-1081.
- [95] Leigh R G and Phillips P Origin of the Mott gap, arXiv:0812.0593.
- [96] Lanzara A, Bogdanov P V, Zhou X J, Kellar S A, Feng D L, Lu E D, Yoshida T, Eisaki H, Fujimori A, Kishio K, Shimoyama J I, Noda T, Uchida S, Hussain Z and Shen Z X 2001 Evidence for ubiquitous strong electron-phonon coupling in high-temperature superconductors Nature **412** 510-514.
- [97] Graf J, Gweon G H, McElroy K, Zhou D Y, Jozwiak C, Rotenberg E, Bill A, Sasagawa T, Eisaki H, Uchida S, Takagi H, Lee D H, and Lanzara A 2007 Universal High Energy Anomaly in the Angle-Resolved Photoemission Spectra of High Temperature Superconductors: Possible Evidence of Spinon and Holon Branches Phys. Rev. Lett. **98** 67004.
- [98] Macridin A, Jarrell, M, Maier, T A, and Scalapino D J (2007) High energy kink in the single

- particle spectra of the two-dimensional Hubbard model Phys. Rev. Lett. **99** 237001/1-4.
- [99] Zemljic M M, Prelovsek P, and Tohyama T (2007) Temperature and doping dependence of high-energy kink in cuprates Phys. Rev. Lett. **100**, 036402/1-4.
- [100] Fisher D S, Kotliar G and Moeller, G 1995 Midgap states in doped Mott insulators in infinite dimensions, Phys. Rev. B **52**, 17112-17118.
- [101] Maier T, Jarrell M, Pruschke T and Hettler M H, 1027 Quantum Cluster Theories **77**, 1028-1090.
- [102] Stanescu T D and Phillips P 2003 Pseudogap in doped Mott insulators is the Near-neighbour analogue of the Mott gap, Phys. Rev. Lett. **91**, 017002/1-4.
- [103] Hwang J, Timusk T and Gu G D, 2007 Doping dependent optical properties of $\text{Bi}_2\text{Sr}_2\text{CaCu}_2\text{O}_{8+\delta}$ J. Phys. Condens. Matter **19** 125208-125240.
- [104] Onose Y, Taguchi Y, Ishizaka K, and Tokura Y 2004 Charge dynamics in underdoped $\text{Nd}_{2-x}\text{Ce}_x\text{CuO}_4$: Pseudogap and related phenomena Phys. Rev. B **69** 024504/1-13.
- [105] Lucarelli A, Lupi S, Ortolani M, Calvani P, Maselli P, Capizzi M, Giura P, Eisaki H, Kikugawa N, Fujita T, Fujita M, and Yamada K 2003 Phase Diagram of $\text{La}_{2-x}\text{Sr}_x\text{CuO}_4$ Probed in the Infrared: Imprints of Charge Stripe Excitations Phys. Rev. Lett. **90** 037002/1-4.
- [106] Cvetkovic V, Nussinov Z, Mukhin S, and Zaanen J, 2007 Observing the fluctuating stripes in high-Tc superconductors Europhys. Lett. **81** 27001-27004.
- [107] Loram J W, Luo J, Cooper J R, Liang W Y and Tallon J L, 2001 Evidence on the pseudogap and condensate from the electronic specific heat J. Phys. and Chem. Sol. **62** 59-64.
- [108] Phillips P and Chamon C 2005 Breakdown of One-Parameter Scaling in Quantum Critical Scenarios for High-Temperature Copper-Oxide Superconductors Phys. Rev. Lett. **95** 107002/1-4.
- [109] Bass J, Pratt W P, and Schroeder P A, 1990 The temperature-dependent electrical resistivities of the alkali metals Rev. Mod. Phys. **62** 645-744.
- [110] Honma T and Hor P H Unified electronic phase diagram for hole-doped high- T_c cuprates 2008 Phys. Rev. B **77**, 184520/1-16.
- [111] Presland J, Tallon J L, Buckley R G, Liu R S and Flower N E, 1991 General trends in oxygen stoichiometry effects on T_c in Bi and Tl superconductors, Physica C **176** 95-105.
- [112] Beni G, 1973 Thermoelectric power of the narrow-band Hubbard chain at arbitrary electron density: Atomic limit Phys. Rev B **10** 2186-2189.
- [113] Chakraborty S, Galanakis D and Phillips P Emergence of particle-hole symmetry near optimal doping in the high-temperature copper-oxide superconductors, arXiv:0807.2854.
- [114] Rübhausen M, Gozar A, Klein M V, Guptasarma P, and Hinks D G, 2001 Superconductivity-induced optical changes for energies of 100Δ in the cuprates Phys. Rev. B **63**, 224514/1-5.
- [115] Santander-Syro A F, Lobo R P S M, Bontemps N, Konstantinovic Z, Li Z Z, and Raffy H 2003 Pairing in cuprates from high energy electronic states Europhys. Lett. **62**, 568-574.
- [116] Molegraaf H J A, Presura C, van der Marel D, Kes P H, and Li M, 2002 Superconductivity-induced transfer of in-plane spectral weight in $\text{Bi}_2\text{Sr}_2\text{CaCu}_2\text{O}_{8+\delta}$ Science, **295** 2239-2241.